Monthly Notices
of the
ROYAL ASTRONOMICAL SOCIETY

Mon. Not. R. Astron. Soc. **401,** 275–293 (2010) doi:10.1111/j.1365-2966.2009.15633.x

The relation between the most-massive star and its parental star cluster mass

C. Weidner,[1,2]★ P. Kroupa[3]★ and I. A. D. Bonnell[1]★

[1]*Scottish Universities Physics Alliance (SUPA), School of Physics and Astronomy, University of St Andrews, North Haugh, St Andrews, Fife KY16 9SS*
[2]*Departamento de Astronomía y Astrofísica, Pontificia Universidad Católica de Chile, Av. Vicuña MacKenna 4860, Macul, Santiago, Chile*
[3]*Argelander-Institut für Astronomie (Sternwarte), Auf dem Hügel 71, D-53121 Bonn, Germany*

Accepted 2009 August 28. Received 2009 August 28; in original form 2009 June 12

ABSTRACT

We present a thorough literature study of the most-massive star, $m_{\rm max}$, in several young star clusters in order to assess whether or not star clusters are populated from the stellar initial mass function (IMF) by random sampling over the mass range $0.01 \leq m \leq 150\,{\rm M}_\odot$ without being constrained by the cluster mass, $M_{\rm ecl}$. The data reveal a partition of the sample into lowest mass objects ($M_{\rm ecl} \leq 10^2\,{\rm M}_\odot$), moderate mass clusters ($10^2\,{\rm M}_\odot < M_{\rm ecl} \leq 10^3\,{\rm M}_\odot$) and rich clusters above $10^3\,{\rm M}_\odot$. Additionally, there is a plateau of a constant maximal star mass ($m_{\rm max} \approx 25\,{\rm M}_\odot$) for clusters with masses between $10^3\,{\rm M}_\odot$ and $4 \times 10^3\,{\rm M}_\odot$. Statistical tests of this data set reveal that the hypothesis of random sampling from the IMF between 0.01 and $150\,{\rm M}_\odot$ is highly unlikely for star clusters more massive than $10^2\,{\rm M}_\odot$ with a probability of $p \approx 2 \times 10^{-7}$ for the objects with $M_{\rm ecl}$ between 10^2 and $10^3\,{\rm M}_\odot$ and $p \approx 3 \times 10^{-9}$ for the more massive star clusters. Also, the spread of $m_{\rm max}$ values at a given $M_{\rm ecl}$ is smaller than expected from random sampling. We suggest that the basic physical process able to explain this dependence of stellar inventory of a star cluster on its mass may be the interplay between stellar feedback and the binding energy of the cluster-forming molecular cloud core. Given these results, it would follow that an integrated galactic IMF (IGIMF) sampled from such clusters would automatically be steeper in comparison to the IMF within individual star clusters.

Key words: stars: formation – stars: luminosity function, mass function – Galaxy: stellar content – galaxies: evolution – galaxies: star clusters – galaxies: stellar content.

1 INTRODUCTION

Whether or not newborn stars in star clusters are randomly drawn[1] from the IMF is of utmost importance for various fields of stellar astrophysics. For example, non-random drawing which suppresses the number of OB stars in smaller clusters would steepen the IMF for whole galaxies, the integrated galactic stellar initial mass function (IGIMF; Kroupa & Weidner 2003; Weidner & Kroupa 2005). A randomly drawn IMF on the other hand, which would be equivalent to postulating the existence of clusters comprised of a massive star and not much more, would not (Elmegreen 2006; Selman & Melnick 2008). As the bulk of the galactic field star populations are probably made from dissolving star clusters (Kroupa 1995; Lada & Lada 1995, 2003; Adams & Myers 2001; Allen et al. 2007), understanding the stellar distribution in galaxies pre-supposes knowledge of the IMF in star clusters. A central issue on deciding whether a star cluster can be modelled in terms of random sampling from the IMF or not is the existence of a non-trivial relation between the mass of the most-massive star ($m_{\rm max}$) and the star cluster mass ($M_{\rm ecl}$). Thus, a statistically significant correlation $m_{\rm max}(M_{\rm ecl})$ would imply physical processes such as self-regulation of the star-formation process in a cluster. The influence of the cluster mass or density on its stellar population has been studied on previous occasions. Larson (1982) and Larson (2003) examined the properties of molecular clouds and the stellar populations found within them, finding the following empirical expression between the mass of the most-massive star, $m_{\rm max}$, and the stellar mass of an embedded cluster, $M_{\rm ecl}$,

$$m_{\rm max}^{\rm Larson} = 1.2 M_{\rm ecl}^{0.45}, \quad (1)$$

which is shown as a dash–dotted line in Fig. 1.

★E-mail: cw60@st-andrews.ac.uk (CW); pavel@astro.uni-bonn.de (PK); iab1@st-andrews.ac.uk (IADB)

[1] Random sampling means choosing a number N of stars randomly from the distribution function which is in this case the IMF.

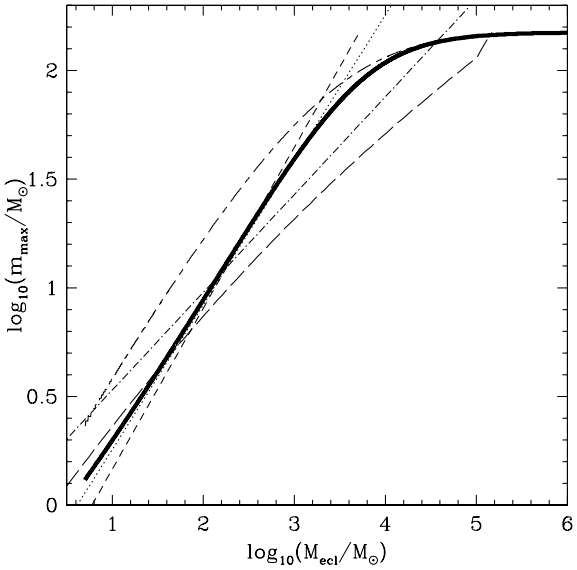

Figure 1. Different relations between the most-massive star and the cluster mass from observations, numerical calculations and theoretical modelling from the literature. The dash–dotted line marks the empirical relation by Larson (2003), the long-dashed line is the Elmegreen (1983) relation, the short-dashed line is the Elmegreen (2000) relation, the dotted line shows the Bonnell et al. (2003) relation, the short-dashed–long-dashed line is the Oey & Clarke (2005) relation and the thick-solid line is the analytical model of Weidner & Kroupa (2004). See text for more details.

Elmegreen (1983) investigated a model for the formation of bound star clusters where the luminosity of the stars chosen from a Miller & Scalo (1979) IMF overcomes the binding energy of a molecular cloud. Different star formation efficiencies would then determine if a cloud becomes a bound star cluster or an OB association. He also found a relation between $m_{\rm max}$ and $M_{\rm ecl}$ which cannot be written as an analytical equation and is shown as a long-dashed line in Fig. 1. Later, Elmegreen (2000) derived a different relation when assuming a single slope power-law IMF, $\xi(m)$, where $\mathrm{d}N = \xi(m)\mathrm{d}m$ is the number of stars in the mass interval $m, m + \mathrm{d}m$, with a Salpeter (1955) slope and solving the following two equations,

$$1 = \int_{m_{\rm max}}^{m_{\rm max*}} \xi(m)\,\mathrm{d}m \tag{2}$$

and

$$M_{\rm ecl} = \int_{m_{\rm min}}^{m_{\rm max}} m\xi(m)\,\mathrm{d}m, \tag{3}$$

but without any limit for masses of the stars, $m_{\rm max*} = \infty$. Here, $m_{\rm min}$ is the minimum mass. For a single power-law IMF with a Salpeter (1955) slope these two equations yield in,

$$m_{\rm max}^{\rm Elmegreen} = \left(\frac{M_{\rm ecl}}{3\times10^3}\right)^{-1.35} \times 100, \tag{4}$$

shown as the short-dashed line in Fig. 1.

In their numerical calculations of star-forming molecular clouds using a smoothed particle hydrodynamics code Bonnell, Bate & Vine (2003), Bonnell, Vine & Bate (2004) found a relation,

$$m_{\rm max}^{\rm Bonnell} = 0.39 \times M_{\rm ecl}^{2/3}, \tag{5}$$

which is shown as a dotted line in Fig. 1.

In a thorough study of star clusters and OB associations in order to determine whether or not a fundamental upper mass limit for stars exists, Oey & Clarke (2005) also calculated the expected dependence of $m_{\rm max}$ on $M_{\rm ecl}$ if the stars are randomly drawn from an IMF,

$$m_{\rm max}^{\rm Oey} = m_{\rm max*} - \int_0^{m_{\rm max*}} \left[\int_0^{M_{\rm ecl}} \xi(m)\mathrm{d}m\right]^N \mathrm{d}M_{\rm ecl}, \tag{6}$$

plotted as a short-dashed–long-dashed line in Fig. 1.

Including a fundamental upper mass limit for stars, $m_{\rm max*} = 150\,\mathrm{M}_\odot$[2] in equations (2) and (3), and using the canonical multipart power-law IMF (Appendix A) Weidner & Kroupa (2004) found the relation visible as a thick-solid line in Fig. 1.

As evident from Fig. 1 these studies arrive at a rather large range of possible $m_{\rm max}$–$M_{\rm ecl}$ relations. Weidner & Kroupa (2006) re-investigated this question by compiling a larger number of observational results from the literature and extensive Monte Carlo experiments of different sampling algorithms and found evidence that there exists a non-trivial relation between the mass of a star cluster and the most-massive star in the cluster, a result in principle confirmed by Selman & Melnick (2008). But they conclude that the Weidner & Kroupa (2006) sample is biased by a size-of-sample effect. Furthermore, in the recent literature several claims have been made against such a relation arguing instead for a pure random sampling from the IMF in individual star clusters (Oey, King & Parker 2004; de Wit et al. 2005; Elmegreen 2006; Parker & Goodwin 2007; Maschberger & Clarke 2008; Selman & Melnick 2008). de Wit et al. (2004, 2005) find upto 4 per cent of non-runaway (less than 30 km s^{-1} space motion) O stars in isolation with no apparent cluster around them or within their lifetime if they would have been ejected from a cluster with a velocity of 6 km s^{-1} – indicating they formed outside a cluster. This result would of course be irreconcilable with a relation between the mass of the most-massive star and the mass of its parent star cluster as has been pointed out by Parker & Goodwin (2007) and Selman & Melnick (2008). While Selman & Melnick (2008) argue that the sample used in Weidner & Kroupa (2006) is biased against random sampling, Parker & Goodwin (2007) find that the observed 4 per cent of allegedly isolated O stars would agree with random sampling from a cluster number distribution function which scales with N^2, where N is the number of stars in a cluster. But it should be noted here that the de Wit et al. (2005) result is an *upper limit* for O stars formed in isolation and that more in-depth observations might reduce this sample. For example, HD 165319, an O9.5 I star from the de Wit et al. (2005) sample of 11 stars which are indicated there as one of 'the best examples for isolated Galactic high-mass star formation' has a bow-shock front and is therefore a star ejected from a star cluster, possibly NGC 6611 (Gvaramadze & Bomans 2008). Additionally, according to Schilbach & Röser (2008) further six of the remaining 10 stars are at distances to star clusters only slightly larger than what they may have travelled during their expected lifetimes. But the current large errors of the space motion of these stars do not allow to constrain the birth places of them.

A non-trivial $m_{\rm max}$–$M_{\rm ecl}$ relation, and therefore whether or not the stars in star clusters are randomly sampled from the IMF, would also give more insight and understanding of the process of star formation. The formation of massive stars ($>10\,\mathrm{M}_\odot$) is still not well understood with at least two competing theories (competitive accretion versus single star accretion) having been developed (Bonnell, Bate & Zinnecker 1998; Bonnell et al. 2004; Bonnell &

[2] $150\,\mathrm{M}_\odot$ is believed to be the fundamental upper mass limit for stars with non-zero metallicity (Weidner & Kroupa 2004; Figer 2005; Oey & Clarke 2005; Koen 2006).

Bate 2006; Tan, Krumholz & McKee 2006; Krumholz et al. 2009). An $m_{\rm max}$–$M_{\rm ecl}$ relation could imply that the bulk of the low-mass stars form first and the high-mass stars later. The combined feedback of the massive stars would then halt further star formation.

Here, we will show that the observed distribution of the mass, $m_{\rm max}$, of the most-massive star in a star cluster cannot be drawn randomly from the IMF for clusters more massive than $100\,{\rm M}_\odot$, but there must exist a physical relation between $m_{\rm max}$ and the birth stellar mass of the cluster, $M_{\rm ecl}$ (the stellar content before gas expulsion but after cessation of star formation).

2 THE DATA

2.1 Sample construction

In order to construct a sufficiently large observational sample to test whether random sampling from the IMF is an acceptable model in star clusters, the available literature was searched for star clusters which are young enough to not to have experienced supernova events and are dynamically rather un-evolved. For the latter, the star clusters should still be embedded in their natal gas cloud or at least be very young, such that gas expulsion would not have effected them strongly (Lada, Margulis & Dearborn 1984; Goodwin 1997; Kroupa, Aarseth & Hurley 2001; Bastian & Goodwin 2006; Goodwin & Bastian 2006; Pellerin et al. 2006; Weidner et al. 2007; Wang et al. 2008). Therefore, only clusters younger than 4 Myr have been included in our sample. Additionally, the young age limits the amount of mass-loss experienced by massive stars due to stellar evolution.

An allegedly suitable sample of objects discussed by Parker & Goodwin (2007) and Maschberger & Clarke (2008) is the one compiled by Testi et al. (1997), Testi, Palla & Natta (1998, 1999) as these authors were explicitly searching for clusters around young A and B stars. We do not use the majority of the clusters from these studies for the following reasons: (a) the majority are too old (>4 Myr for 25 of 35 objects) or they are (b) gas free. The age limit imposed here is given by the short lifetime of massive stars and to limit stellar mass loss of the massive stars. Completely gas-free objects are unsuited for the task of this work as gas expulsion will remove large amounts of stars and therefore reduce the mass of the cluster, $M_{\rm ecl}$, significantly (Kroupa et al. 2001; Weidner et al. 2007). The exception are four objects which this sample has in common with the near infrared study of young star-forming regions by Wang & Looney (2007) and which are all included in our study. Based on similar arguments Maschberger & Clarke (2008) also excluded the Testi et al. (1997, 1998, 1999) sample from their final statistical analysis.

A very recent additional sample is provided by Faustini et al. (2009). The authors study 26 high-luminosity *IRAS* sources and find that 22 of them show evidence for clustering. They model nine of these clusters in order to derive cluster masses and the mass of the most massive stars. This sample is included in our study too. But because the results are based on modelling, different symbols for them are used in subsequent plots. Faustini et al. (2009) conclude that the masses of the most-massive star in these clusters are also not reconcilable with random sampling of the stars from the IMF.

2.2 Mass of a cluster versus number of stars in a cluster

The claim has been made (Parker & Goodwin 2007; Maschberger & Clarke 2008) that the number of stars within a star cluster, $N_{\rm ecl}$, gives a better statistical description of the cluster compared with the cluster mass, $M_{\rm ecl}$, because $N_{\rm ecl}$ is an observed quantity and statistically more easily manageable. This is, however, not entirely true as observational biases handicap $N_{\rm ecl}$ to a larger extent than $M_{\rm ecl}$. As the lower mass limit of the observations depend on telescope time, distance of the object, reddening and observed colour range, the different clusters have to be normalized to the same lower mass limit in order to make them comparable. This is done for $N_{\rm ecl}$ in the same way as for $M_{\rm ecl}$ – by extrapolating the stars in the observed mass range to a general mass range (0.01–$150\,{\rm M}_\odot$ in this study) with the use of an IMF. Therefore, $N_{\rm ecl}$ is *not* an observed quantity but an estimated one. But the sources for potential error are much larger in the case of $N_{\rm ecl}$ than compared with $M_{\rm ecl}$, as the observed number of stars gives every star the same statistical weight, regardless if it is an M dwarf or an O supergiant. But low-mass stars and brown dwarfs are easy to miss due to being faint but also due to unresolved binarity and crowding of stars (Maíz Apellániz 2008; Weidner, Kroupa & Maschberger 2009). Very young low-mass pre-main sequence (PMS) stars and brown dwarfs are still difficult to model because they are dominated by the unknown accretion history, and magnetic fields and fast rotation have a strong influence (Chabrier, Gallardo & Baraffe 2007; Ribas et al. 2008). Therefore is the observational lower mass limit highly model-dependent and has large errors. Because the IMF is dominated in number by low-mass objects (85 per cent of all stars are below $0.5\,{\rm M}_\odot$ for the IMF described in Appendix A) uncertainties in the lower mass limit severely affect the $N_{\rm ecl}$ estimate. The mass, $M_{\rm ecl}$, in contrast is far easier to estimate by the number of high-mass stars (Maíz Apellániz 2009). Likewise, the stellar evolution models of massive stars still include large uncertainties. As in the case of low-mass stars, the effects of fast rotation and magnetic fields in these stars are not well understood. Massive stars are small in numbers (6 per cent of all stars are above $1\,{\rm M}_\odot$) but dominate the cluster in mass (50.7 per cent of the total mass is in stars above $1\,{\rm M}_\odot$ for a cluster comprised of 0.01–$150\,{\rm M}_\odot$ objects according to the canonical IMF as described in Appendix A). Because of the intrinsic brightness of these objects, they are easy to access observationally and difficult to miss. While the binary frequency might be lower for low-mass stars (∼35 per cent) compared to massive stars (20–80 per cent, Garmany, Conti & Massey 1980; García & Mermilliod 2001; De Becker et al. 2006; Lucy 2006; Apai et al. 2007; Kiminki et al. 2007; Sana et al. 2008; Turner et al. 2008; Weidner et al. 2009), the effect of unresolved binaries is smaller for the mass estimate than for the number estimate. If all stars were in unresolved binaries, $N_{\rm ecl}$ would miss 50 per cent of the stars while $M_{\rm ecl}$ would miss only 16–30 per cent, depending on the mass-ratio distribution (Weidner et al. 2009). We therefore choose to study $m_{\rm max}$ in dependence of $M_{\rm ecl}$ rather than $N_{\rm ecl}$.

2.3 Additional issues

If gas-expulsion already starts early on, before the explosion of supernovae, even the young objects presented here might be affected by mass loss due to the unbinding of stars from the cluster.

One possible additional effect which might deplete very young star clusters especially from massive stars is dynamical ejections after stellar encounters in the dense decoupled cores of massive clusters (Clarke & Pringle 1992; Pflamm-Altenburg & Kroupa 2006). Unfortunately, this effect is impossible to avoid or to correct for reliably and might lead to an additional underestimation of the cluster masses, but it is unlikely that the most-massive star is ejected from the cluster.

Already in Weidner & Kroupa (2006), a first set of young star clusters and their most massive stars were presented. In the current

Table 1. For these massive stars in star clusters dynamical mass estimates exist from the orbits of binaries.

Cluster	Star	Sp Type	$m_{\rm dynamical}$ $M_\odot$	$m_{\rm old}$ $M_\odot$	$m_{\rm new}$ $M_\odot$	$m_{\rm ini\,new}$ $M_\odot$	Ref.
Trumpler 14/16	FO15B	O9.5V	16.0 ± 1.0	23.3 ± 2.0	16.5 ± 1.5	$17.9\ -3.9/+3.1$	(1)
Trumpler 14/16	FO15A	O5.5V	30.0 ± 1.0	50.4 ± 6.0	34.2 ± 3.0	$37.7\ -3.7/+7.3$	(1)
M42	Θ Orionis C1	O6Vpe	35.8 ± 7.2	45.0 ± 5.0	31.7 ± 6.0	$34.3\ -4.3/+4.7$	(2)
Trumpler 14/16	HD93205A	O3V	56.0 ± 4.0	87.6 ± 12.0	58.3 ± 10.0	$64.6\ -4.6/+5.4$	(3)
Westerlund 2	WR20a A	WN6ha	82.7 ± 5.5	-	-	$121.0\ -41.0/+29.0$	(4)
NGC3603	NGC3603-A1	WN6ha	116.0 ± 31	120.0 ± 15.0	-	$121.0\ -41.0/+29.0$	(5)

(1) Niemela et al. (2006), (2) Kraus et al. (2009), (3) Morrell et al. (2001), (4) Nazé et al. (2008), (5) Schnurr et al. (2008).

contribution the Weidner & Kroupa (2006) list is included, corrected for a few errors and significantly expanded. The sample of 100 both new and previously published star clusters is shown as Table B1 in Appendix B. The table shows two mass values for the mass of the most-massive star. The one in Column 3 is based on the Vacca, Garmany & Shull (1996) spectral class to stellar mass conversion. In Column 4, additionally, a new spectral class to mass conversion is used. It is based on Martins, Schaerer & Hillier (2005) and Martins & Plez (2006) who provide two new transformations of O-star spectral types into masses, which are both rather similar. One is based on a theoretical effective temperature scale and the other on an observational one. The authors note that their new calibration should represent a significant improvement over previous calibrations, due to the detailed treatment of non-local thermodynamic equilibrium line blanketing in their calculations. Using the new transformation based on the theoretical effective temperature scale (table 1 in Martins et al. 2005), all the clusters with O stars ($m \gtrsim 16\,M_\odot$) in Table B1 are re-examined. The resulting new spectral masses are corrected for stellar evolutionary effects (Weidner 2009) and the new masses for the most-massive stars are compiled in Column 4 of the same table. The difference between the old and the new calibration is visualized in Fig. B1 in Appendix B. As is shown there, in all but four cases the new calibration results in stellar masses significantly lower than the old values. Note that the new calibration by Martins et al. (2005) is only provided up to a spectral type of O3. This might not include the most massive stars observed but no general consensus exists in spectral classifying of extremely massive stars. While, traditionally they would be of spectral type O3 some classify them as spectral type O2 or even earlier (Walborn et al. 2002) while others prefer a Wolf–Rayet star classification (for example WN6h; Crowther 2007). In these cases the corrected values based on the Crowther (2007) Wolf–Rayet scheme in Weidner (2009) are used.

An additional complication in the determination of the masses of the most-massive stars is due to possible binary stellar evolution (BSE). Massive stars are often found in close binaries of rather similar masses (Weidner et al. 2009) and therefore BSE might have affected the evolution and hence the observational parameters of the stars (Wijers, Davies & Tout 1996; Tout et al. 1997; Hurley 2003; Zhang et al. 2005).

Except for a few cases the cluster masses are derived by extrapolating from the given number of stars above a certain mass limit or within certain limits to a mass range of 0.01–150.0 $M_\odot$ with a canonical IMF (see Appendix A).

Several cluster masses given in Carpenter et al. (1993) are used as lower limits only in this study because of incompleteness and uncertain differential reddening.

In Appendix C, notes on some individual clusters can be found.

2.4 Dynamical masses

In recent years, observational techniques allowed to measure masses of very massive stars directly by observing the orbits of massive eclipsing binaries. In Table 1, the dynamical mass estimates for six very massive stars are compared with old and new spectroscopic estimates. Two of these six stars (WR20a A and Θ Orionis C1) happen to be the most massive stars in two clusters (Westerlund 2 and M42). Also shown in Table 1 are the initial masses for these stars, $m_{\rm ini\,new}$, derived by matching the luminosity and effective temperature of the newly calibrated O star spectral types by Martins et al. (2005) with the values from the Meynet & Maeder (2003) rotating stellar evolution models for massive stars (for details see Weidner 2009). Generally, the new spectroscopic mass estimates from the new calibration agree much better with the dynamical masses than the old spectroscopic mass estimates. For the analysis done in this work for WR20a A and Θ Orionis C1, the dynamical masses are used for the old calibration and $m_{\rm ini\,new}$ for the new one.

2.5 The cluster sample

Table B1 in Appendex B includes the Weidner & Kroupa (2006) sample of most-massive stars in star clusters together with the new entries compiled here from the literature. Fig. 2 shows the most-massive star versus star-cluster mass relation from this table using the old stellar masses for the O stars. Furthermore, the figure shows the theoretical analytic result (the thick solid line) from Weidner & Kroupa (2004), which numerically solves equations (2) and (3) but with the canonical multipart power-law IMF and assuming a fundamental upper mass limit for stars, $m_{\rm max*} = 150\,M_\odot$ to arrive at a relation for $m_{\rm max} = f_{\rm ana}(M_{\rm ecl})$.

The masses of the most-massive stars derived from the new spectral type to mass conversion are shown in Fig. 3 together with the same lines as in Fig. 2.

2.5.1 Errors

The error bars for $M_{\rm ecl}$ in Table B1 are either directly taken from the respective literature source or by assuming an uncertainty of 100 per cent in the number of observed stars. For $m_{\rm max}$, the errors are again taken either directly from the literature or the spectral type is converted to mass by the Vacca et al. (1996) tables for Column 3 and Martins et al. (2005) for Column 4[3] and the spectral subtype $+1$ and -1 is used as the upper and lower limit for the stellar

[3] The masses are corrected for stellar evolutionary effects as described in Weidner (2009).

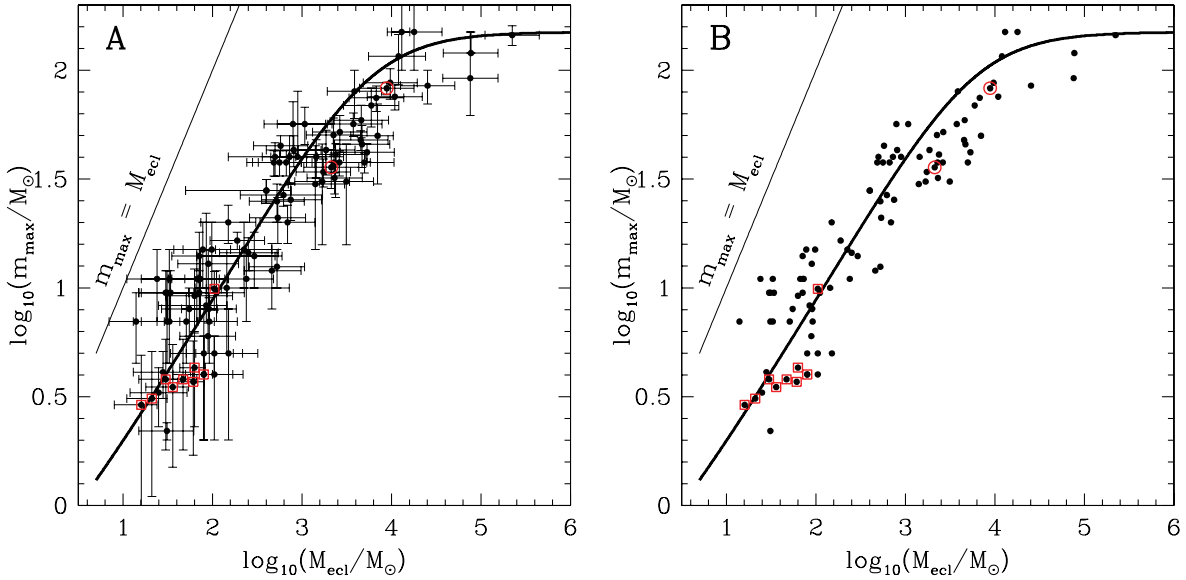

Figure 2. Plot of the most-massive star versus star-cluster mass data using the literature values for the stellar masses and the old effective temperature scale calibration for O stars. Panel A: with error bars and Panel B without error bars. The thick solid line represents the analytic model from Weidner & Kroupa (2004), see also Fig. 1. The literature values with circles around them have dynamical mass estimates for the most-massive star while the ones with boxes are the sample of Faustini et al. (2009) for which the masses of the most-massive stars are only indirectly calculated. The thin solid line marks the identity when a cluster is made of only one star.

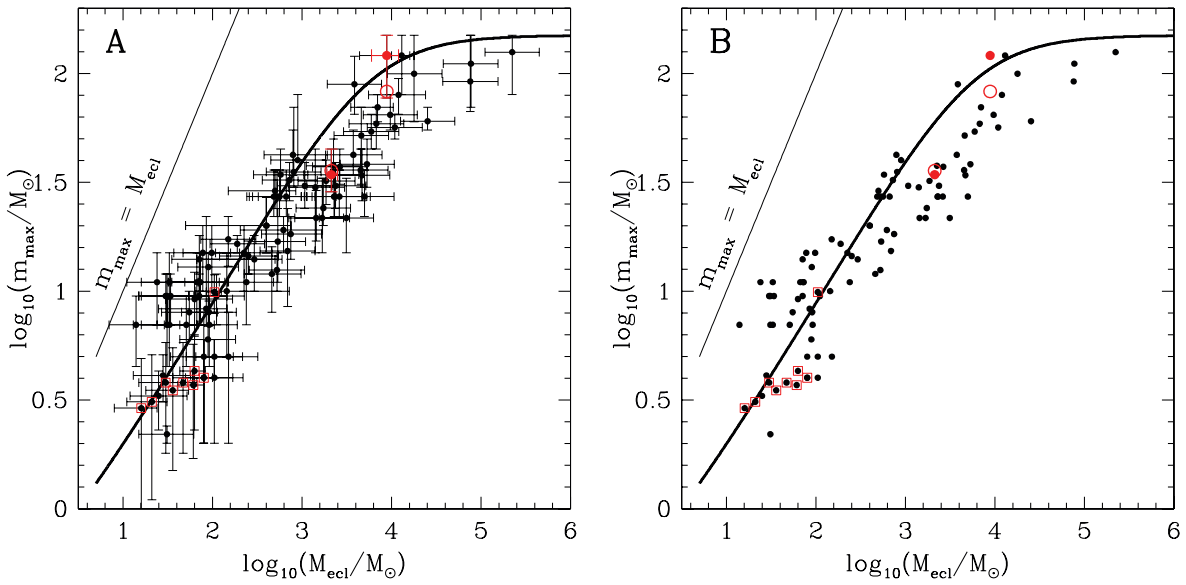

Figure 3. Like Fig. 2 but using the new effective temperature-scale calibration for O stars from Martins et al. (2005) corrected for evolutionary effects to initial masses (Weidner 2009). Panel A: with error bars and Panel B without error bars. The dynamical mass estimates are shown only as open circles as the evolutionary corrected initial masses are used for the actual analyses.

mass,[4] respectively. The errors in the distance and age are from the literature only.

3 STATISTICAL ANALYSES

In the supplement of Pflamm-Altenburg & Kroupa (2008), the probability for the ith massive star randomly chosen from a number of stars N is given, assuming $m_{\max *} = 150\,\mathrm{M}_\odot$. For $i = 1$ (the most-massive star) the probability is

$$p_{N(m)} = N \left(\int_{m_{\min}}^{m} \widetilde{\xi}(m)\,\mathrm{d}m \right)^{N-1} \widetilde{\xi}(m), \qquad (7)$$

with $\widetilde{\xi}(m) \propto \xi(m)$ being the probability density distribution and $\xi(m)$ the IMF as described in Appendix A.

In order to get the number of stars, N, required for equation (7) for a given cluster with $M_{\rm ecl}$, an array of cluster masses between $5\,\mathrm{M}_\odot$ and $10^6\,\mathrm{M}_\odot$ is divided by the mean mass, $m_{\rm mean}$, of the IMF. For

[4] For example, for an O4 V star the spectral types O5 V and O3 V are used to determine the lower and upper mass limit.

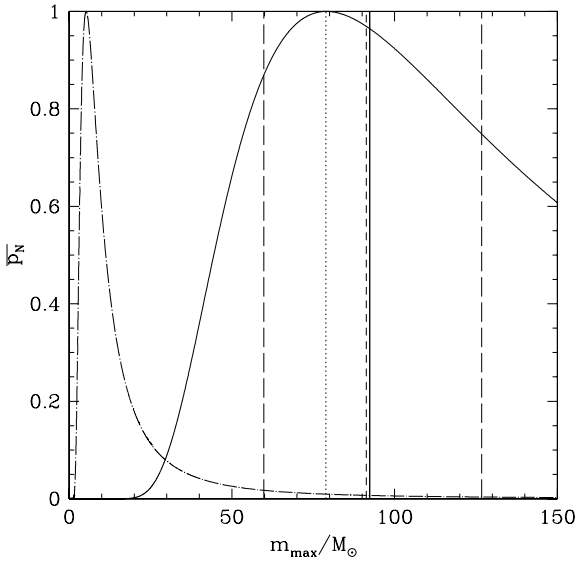

Figure 4. The solid line shows the distribution of the most-massive star for $N = 11111$ ($M_{ecl} \approx 4000\,M_\odot$) and the dash–dotted line is the same for $N = 278$ ($\approx 100\,M_\odot$) according to equation (7). In this plot, p_N is normalized to 1 at the most common (mode) value in order to give both curves the same height. For the $N = 11111$ case, the following statistical properties are also shown: the vertical dotted line is the mode, the vertical dashed line is the median, the vertical solid line is the expectation value and the two vertical long-dashed lines mark the 1/6th and 5/6th quantiles. See text for further details.

the IMF used here (see appendix A for details) $m_{mean} = 0.36\,M_\odot$, if $m_{min} = 0.01\,M_\odot$ and $m_{max*} = 150\,M_\odot$.

Fig. 4 shows the distribution obtained by random sampling (equation 7) for two examples of $N = 278$ (dash–dotted line) and $N = 11111$ (solid line). For each N, the five statistical values are calculated.

(i) The arithmetic mean or expectation value, marked as a solid vertical line for the $N = 11\,111$ case in Fig. 4, is the sum of all most-massive stars divided by the number of clusters.

(ii) The mode value (dotted vertical line in Fig. 4) marks the most common value (the peak in Fig. 4) of the distribution.

(iii) The median value (dashed vertical line in Fig. 4) is the value which divides the distribution in two. 50 per cent of the values are above the median while 50 per cent are below.

(iv) The 1/6th quantile (the left long-dashed vertical line in Fig. 4) is the value below which 1/6th of data points lie.

(v) The 5/6th quantile (the right long-dashed vertical line in Fig. 4) is the value above which 5/6th of data points lie.

The 1/6th and 5/6th quantiles define the region within which lie two thirds of the most-massive stars lie for random sampling of stars from the IMF (equation 7).

3.1 Completeness of the sample

The completeness of the cluster sample presented here strongly depends on the total number of star clusters expected for the Milky Way (MW) which are younger than 4 Myr. This depends on the assumed current star-formation rate (SFR) of the MW (0.8–13 $M_\odot\,yr^{-1}$; Diehl et al. 2006, and references therein), the slope of the embedded cluster mass function ($\beta = 1.8$–2.3; Lada & Lada 2003), where $dN_{ecl} = M_{ecl}^{-\beta}\,dM_{ecl}$ is the number of just formed embedded clusters with stellar mass in the interval $M_{ecl}, M_{ecl} + dM_{ecl}$, and the assumed lower mass limit for star clusters (5–100 $M_\odot$; Weidner & Kroupa 2006). With the observationally favoured parameters being $SFR = 4.0\,M_\odot\,yr^{-1}$, $\beta = 2.0$ and $M_{ecl\,min} = 5\,M_\odot$. The total number of young star clusters in the MW lies therefore between 10^4 and 10^6 clusters. The majority of these have masses less than $100\,M_\odot$ and any surveys of them are severely incomplete. For a completeness estimate, we therefore restrict ourselves to clusters more massive than $1000\,M_\odot$ as they are far fewer in numbers and more easily identified in the MW. For the whole range of parameters of the MW the number of young star clusters more massive than $1000\,M_\odot$ lies somewhere between 160 and 4452, with 1478 being the value for the observationally favoured parameters. The sample shown in Table B1 includes 30 ($-5/+6$) clusters which are in the MW and more massive than $1000\,M_\odot$ within the uncertainties. This suggests that between 18.8 per cent ($-3.1/+3.7$) and 0.7 per cent (± 0.1) of all such clusters are in the sample, with 2.0 per cent ($-0.3/+0.4$) for the favoured parameters. Therefore, one has to keep in mind that any statistical results are possibly limited by the incompleteness of the cluster sample.

3.2 Statistical tests

In panel A of Fig. 5 the mode, mean, median and 1/6th and 5/6th quantiles for a fundamental upper mass limit of $m_{max*} = 150\,M_\odot$ are shown together with the data points from Column 4 and the clusters from Column 3 from Table B1 which have not been changed by the recalibration.

Three different statistical tests are applied to the data in order to verify whether or not the observed most-massive stars are consistent with being randomly drawn from the IMF.

3.2.1 Percentage of stars between the 1/6th and 5/6th quantiles

As is visible in this Fig. 5, there is a general change in behaviour of the data points around a cluster mass of about $100\,M_\odot$ and around $1000\,M_\odot$ with respect to what is expected from random sampling. Below the $100\,M_\odot$ limit the data show a larger spread while above $1000\,M_\odot$ the slope of the m_{max}–M_{ecl} relation changes. Panel A of Fig. 6 shows the percentage of the most-massive stars within the 1/6th and 5/6th quantiles in three samples, one for the clusters below $100\,M_\odot$, one for the clusters between 100 and $1000\,M_\odot$ and one for the ones above $1000\,M_\odot$. Additionally, the figure shows the same numbers for different assumptions on the fundamental upper mass limit (m_{max*}) for stars. Here, the clusters above $1000\,M_\odot$ (filled and open triangles) are far below the 2/3rd range which would be expected from random sampling. The clusters below $100\,M_\odot$ (filled and open circles) and the intermediate clusters (100–$1000\,M_\odot$, filled and open squares) are very tightly within the 1/6th and 5/6th quantiles. About 90 and 78 per cent of the clusters are within the range, respectively. In Panel B of Fig. 6, the same is shown but including the error bars for m_{max} and M_{ecl} from Table B1 by making the same calculations as before but using the minimal and maximal values for m_{max} and M_{ecl}. The low-mass clusters are still more tightly distributed within the 1/6th and the 5/6th quantiles than expected. The intermediate- and high-mass clusters seem to be consistent with random sampling when the maximum effect of the errors is applied to the data.

3.2.2 Distribution around the Median

Also important is the distribution of the $m_{max\,obs}$ values around the median of the expected distribution for random sampling. The median is the statistical value for which 50 per cent of the data should

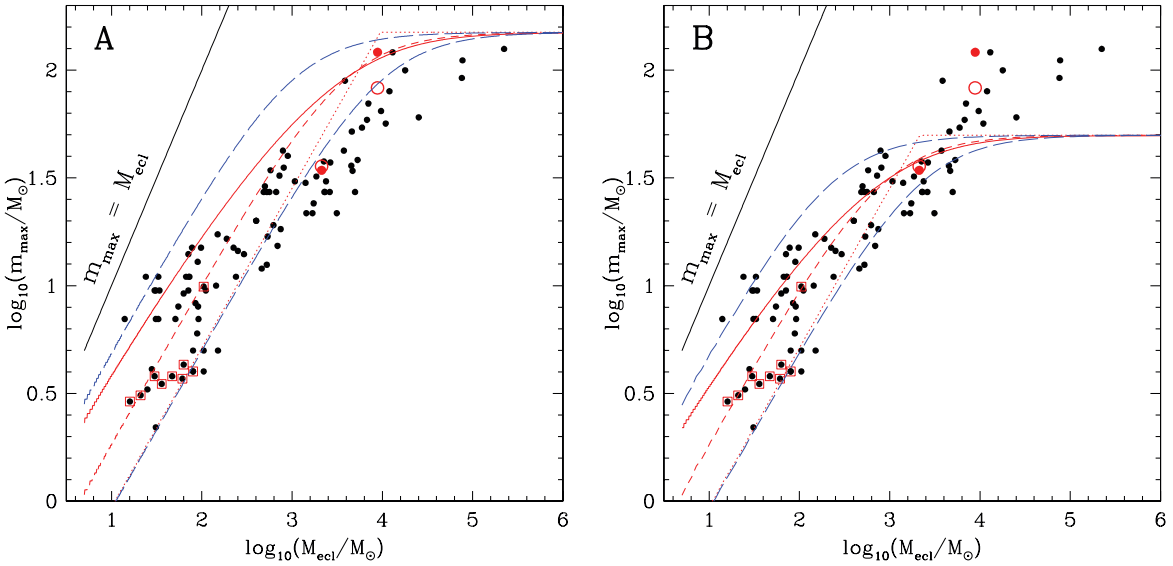

Figure 5. Panel A: most-massive star versus cluster mass. The dots are the observed values from Column 4 from Table B1. The two open circles indicate existing dynamical estimates for the present-day mass of the most-massive stars. The boxed data are from the sample of Faustini et al. (2009). The dotted line refers to the mode value for random sampling, the short-dashed line to the median value, the curved solid line marks the mean value and the two long-dashed lines are the 1/6th (lower) and 5/6th (upper) quantiles between which 2/3rd of the data points should lie if they were randomly sampled from the IMF over the mass range 0.01 $M_\odot$ to $m_{max*} = 150\,M_\odot$. The thin solid line to the left marks the identity where the cluster is made-up only of one star. Panel B: the same as Panel A but assuming a fundamental upper mass limit for stars of $m_{max*} = 50\,M_\odot$ instead of $150\,M_\odot$.

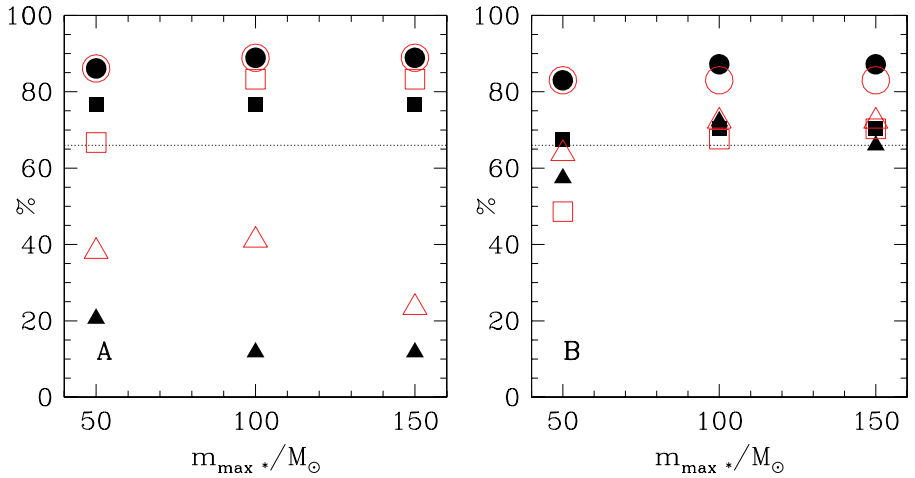

Figure 6. Percentage of most-massive stars within the 1/6th to 5/6th quantiles for three different assumptions of the fundamental upper mass limit, m_{max*}, of 50, 100 and 150 $M_\odot$. Solid symbols refer to the new O-star calibration in Table B1 and open symbols to the old one. Circles mark the percentages for clusters below $10^2\,M_\odot$ while squares are for $100 < M_{ecl} \leq 10^3\,M_\odot$ and triangles mark clusters more massive than $10^3\,M_\odot$. Panel A: these values do not take into account the errors in M_{ecl} and m_{max} in Table B1 while in panel B these errors are included. The horizontal dotted line at 66 per cent marks the fraction of stars that ought to lie between the 1/6th and 5/6th quantiles if random sampling between 0.01 $M_\odot$ and m_{max*} was true.

lie above and below. For the whole sample, 25.7 per cent are above the median and 74.3 per cent below if one uses the new Martins et al. (2005) O-star mass scale and assumes a fundamental upper mass limit of $m_{max*} = 150\,M_\odot$. In the subsample of clusters below $100\,M_\odot$, there are 56.8 per cent above and 43.2 per cent below the median, for the clusters with $100 < M_{ecl} \leq 1000\,M_\odot$ there are 13.3 per cent above and 86.7 per cent below the median, while for the high-mass clusters 2.9 and 97.1 per cent are above and below the median, respectively. In Fig. 7, the distribution of $m_{max\,median} - m_{max\,obs\,new}$ is shown for the whole cluster sample (Panel A) and for the clusters below $10^3\,M_\odot$ (Panel B). For the old O-star mass scale, the distribution is shown in Fig. 8. The percentages in the case of the old O-star mass scale are 35.6/64.4 per cent for the total sample and 56.8/43.2, 40.0/60.0 and 8.8/91.2 per cent for, respectively, the clusters below $100\,M_\odot$, the clusters with $100 < M_{ecl} \leq 1000\,M_\odot$ and the clusters above $10^3\,M_\odot$.

3.2.3 Wilcoxon Signed-Rank Test

The Wilcoxon signed-rank test (Bhattacharyya & Johnson 1977)[5] tests whether or not the data are consistent with being symmetrically distributed around the median. It reveals for the new calibration a

[5] A short introduction into the test and pre-calculated tables for the probabilities for different N can be found at: http://comp9.psych.cornell.edu/Darlington/index.htm

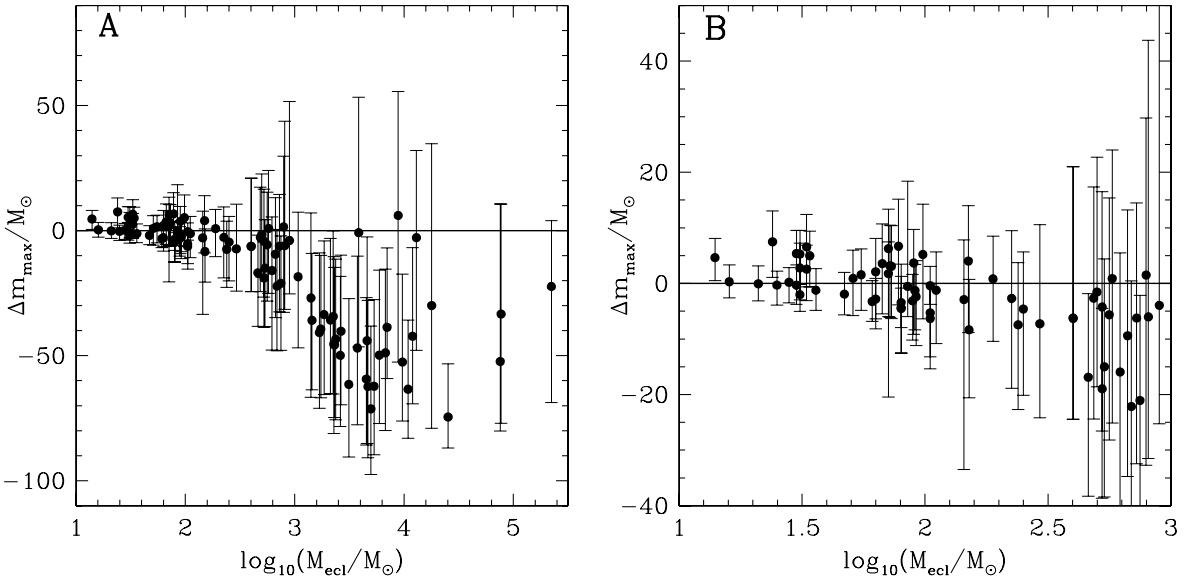

Figure 7. Distance of the observed most-massive star from the expected median for random sampling up to $m_{max*} = 150\,M_\odot$. Here, the new Martins et al. (2005) mass scale is used for O stars. Panel A show the whole sample while panel B contains only the clusters below $10^3\,M_\odot$. For random sampling over the mass range 0.01–150 $M_\odot$ the data ought to be distributed symmetrically about $\Delta\, m_{max} = 0$.

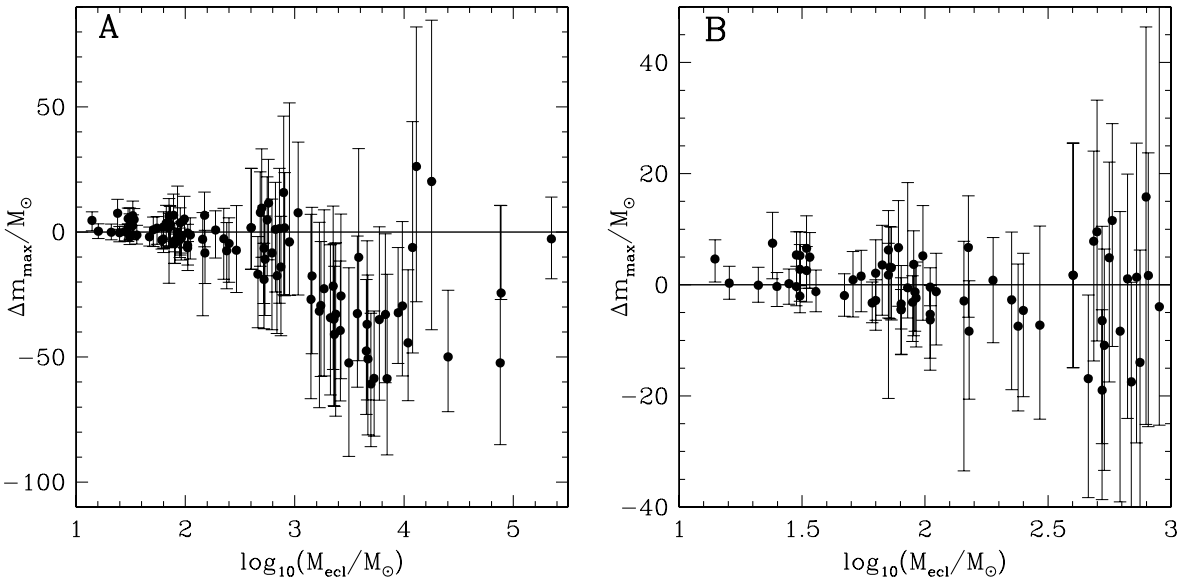

Figure 8. Like Fig. 7 but for the old O-star calibration.

probability.[6] $p(M_{ecl} \leq 100\,M_\odot)$ of 0.014 for clusters with masses smaller or equal to $100\,M_\odot$, a $p(100\,M_\odot < M_{ecl} \leq 1000\,M_\odot)$ of 1.9×10^{-7} for cluster masses between 100 and $1000\,M_\odot$ and a $p(M_{ecl} > 1000\,M_\odot)$ of 2.8×10^{-9} for the clusters above $1000\,M_\odot$. For the old calibrations the probabilities are $p(M_{ecl} \leq 100\,M_\odot) = 0.014$, $p(100\,M_\odot < M_{ecl} \leq 1000\,M_\odot) = 0.035$ and $p(M_{ecl} > 1000\,M_\odot) = 1.2 \times 10^{-8}$.

3.3 Dependence on the high-mass IMF slope

The general assumption in this paper, that the stars in a star cluster follow a universal IMF which is characterized by a Salpeter/Massey slope of 2.35 for all stars above $0.5\,M_\odot$, is strongly supported by almost all observational evidence (see Appendix A for a list of references). However, if the IMF slope for high-mass stars is steeper than 2.35, it is not sure whether or not a fundamental upper mass limit exists, as was pointed out by Oey & Clarke (2005). Fig. 9 shows the mean, median, mode, 1/6th and 5/6th quantiles for two different assumptions of the high-mass slope of the IMF. In Panel A, the slope for stars more massive than $25\,M_\odot$ is changed to $\alpha_3 = 3.0$ and in Panel B to $\alpha_3 = 4.1$, while $\alpha_2 = 2.35$ for stars between 0.5 and $25\,M_\odot$ in both cases. $25\,M_\odot$ was chosen because it is the m_{max} value of the plateau like feature for clusters with masses between 10^3 and $4 \times 10^3\,M_\odot$. Only for a slope as steep as $\alpha_3 = 4.1$ are 50 per cent of stars above and below the median. A slope steeper than $\alpha_3 = 3.7$ is needed in order to have more than 60 per cent of the stars within the 1/6th and 5/6th quantiles. Such steep slopes

[6] ∼0.1 is the highest probability the Wilcoxon signed-rank test allows for.

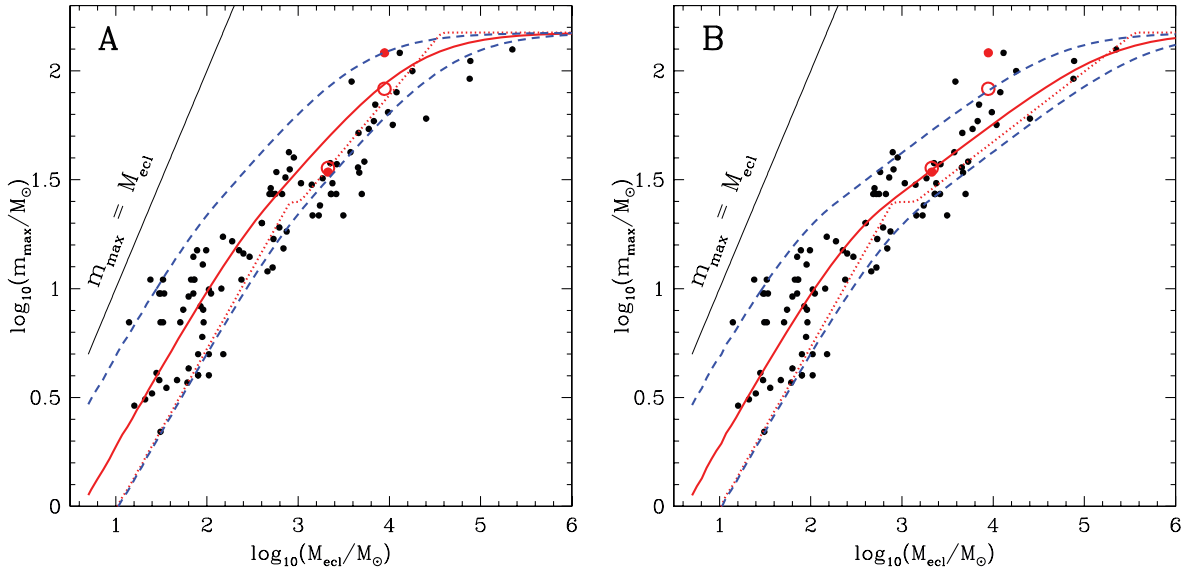

Figure 9. Like Fig. 5 but the IMF slope above 25 $M_\odot$ is 3.0 (Panel A) and 4.1 (Panel B) instead of the Salpeter value of 2.35. The solid line is the median, the dotted line is the mode and the dashed lines are the 1/6th (lower) and the 5/6th (upper) quantiles.

for the high-mass IMF within star clusters are clearly ruled out by the current state of observations (Massey 1998; Elmegreen 1999; Kroupa 2001; Larson 2002b).

3.4 Dependence on the environment

Very recently, Pfalzner (2009) studied the dissolution behaviour of young (1–20 Myr) massive star clusters (2000–50 000 $M_\odot$). She found that her sample of 23 clusters can be divided into two groups, loose clusters ($R_{ecl} > 1$ pc) and tight clusters ($R_{ecl} < 1$ pc), where R_{ecl} is her estimated cluster radius. The radii of the groups each follow a rather tight sequence with time. While the tight clusters expand from ∼0.5 to 3 pc, the loose ones evolve from 4 to 20 pc on the same time-scale, parallel to the tight ones. Of these 23 clusters, 10 are included in our cluster sample. Five of them are tight clusters ([OBS 2003] 179, Westerlund 2, NGC 3603, Trumpler 14, Arches) and five are loose ones (NGC 7380, NGC 2244, IC 1805, NGC 6611, Cyg OB2). When comparing the most-massive stars against the cluster mass of these two subsets, as is done in Fig. 10, it seems that the clusters which form tighter and are therefore more dense, have on an average a more massive maximal star, while the loose clusters prefer less massive maximal stars. For the tight subset a linear function can be fitted with a slope of 0.09 ± 0.39 and a rather low linear correlation coefficient of 0.35 ± 0.47. The slope for the loose sample is 0.27 ± 0.16, somewhat steeper than for the tight sample within the error bars, but the linear correlation coefficient is much larger, about 0.92 ± 0.08. The combined sample has a slope of 0.22 ± 0.23 with a linear correlation coefficient of 0.52 ± 0.47. Therefore, the difference in slopes might be indicating a physical dependence of the mass of the most massive star not only on the cluster mass (previous sections) but also on the cluster density. But the large error bars make a more definite statement difficult. Also it should be noted here that the R_{ecl} estimates for the all the loose clusters of the Pfalzner (2009) sample are the measured median distances of early B type stars in theses clusters (Wolff et al. 2007) and therefore might not be directly comparable to radii arrived at with different methods.

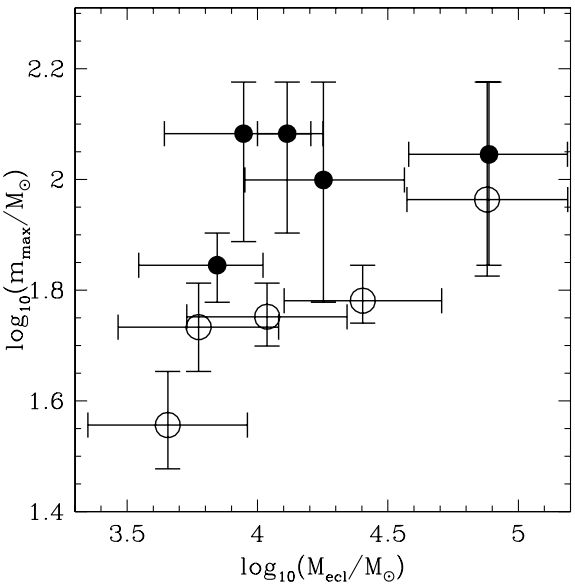

Figure 10. Like Fig. 3 but only the clusters which are in common with the Pfalzner (2009) sample. Filled circles are clusters with radii smaller than 1 pc while the open circles are the clusters with larger radii.

Low-mass young clusters are found to be generally small ($\lesssim$1 pc, Testi, Palla & Natta 1998; Gutermuth et al. 2005; Testor et al. 2005; Rathborne, Jackson & Simon 2006; Scheepmaker et al. 2007) so it is unclear if and how such a correlation between the most-massive star and the cluster radius extends to lower masses.

3.5 A simple model

A simple yet sufficient model to describe the plateau of most-massive stars between 1000 and 4000 $M_\odot$ and the behaviour at higher cluster mass might be the following. The model assumes that the mass of the most-massive star is linked to the proto cluster mass due to stellar feedback. For a range of cluster masses,

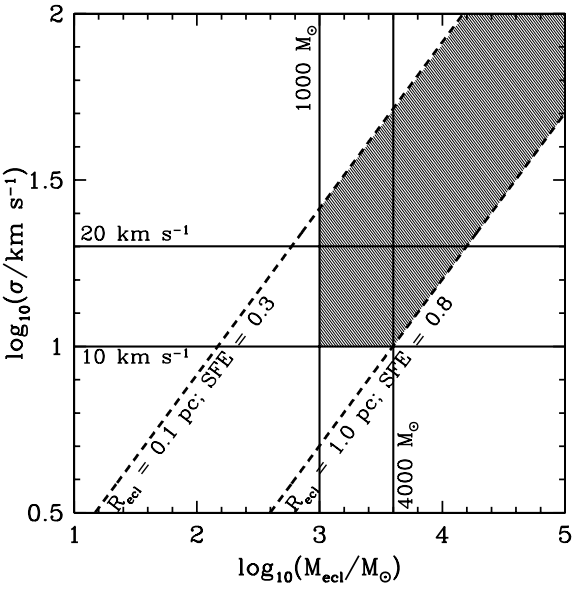

Figure 11. The dashed lines show the dependence of the velocity dispersion, σ, in the cluster on $M_{\rm ecl}$ for a range of cluster radii (0.1–1 pc) and star-formation efficiencies (0.3–0.8). The horizontal lines mark the typical range of velocities for ionized gas, $v_{\rm ion}$ (10–20 km s^{-1}), while the vertical lines are the plateau of most-massive stars for $M_{\rm ecl}$ from 1000 to 4000 M$_\odot$. In the shaded region are lying models for which σ is larger than $v_{\rm ion}$ and $M_{\rm ecl}$ is larger than 1000 M$_\odot$.

$M_{\rm ecl}$ (10–10^6 M$_\odot$), cluster radii, $R_{\rm ecl}$ (from 0.1 to 1.0 pc), and star-formation efficiencies (SFEs) (0.3–0.8), the velocity dispersion, σ, is calculated by

$$\sigma = \sqrt{\frac{3\pi G}{2}\frac{M_{\rm ecl}}{R_{\rm ecl}\,{\rm SFE}}}, \qquad (8)$$

where G is Newton's gravitational constant and SFE $= M_{\rm ecl}/(M_{\rm ecl} + M_{\rm gas})$, with $M_{\rm gas}$ being the residual gas mass in the cluster forming volume.

Fig. 11 shows σ within the proto-cluster as a function of $M_{\rm ecl}$. It is compared with the typical velocity of ionized gas, $v_{\rm ion}$, which is about 10–20 km s^{-1}. As is visible in Fig. 11, σ is larger than $v_{\rm ion}$ for clusters with masses larger than a couple of hundred M$_\odot$, regardless of the radii and SFEs. Therefore, it seems possible that such clusters are able to retain the ionized gas longer – allowing the stars to accrete further mass. The fact that σ already overcomes $v_{\rm ion}$ at rather low $M_{\rm ecl}$ for small $R_{\rm ecl}$ and low SFE can be seen as an indication that low-mass clusters might have lower SFEs than massive clusters.

4 RESULTS AND DISCUSSION

We have studied the possible dependence of the mass of the most-massive star, $m_{\rm max}$, on the stellar mass, $M_{\rm ecl}$, of the host birth cluster. To this effect, we have significantly increased the data sample $m_{\rm max}(M_{\rm ecl})$.

Using the new spectral-type stellar-mass conversion from Martins et al. (2005) and the here presented sample of most-massive stars in star clusters, it has been shown here that the observed sample divides into three subsamples, the first being clusters with $M_{\rm ecl} < 100\,{\rm M}_\odot$, followed by clusters between 100 and 1000 M$_\odot$ and clusters with $M_{\rm ecl} > 1000\,{\rm M}_\odot$. Furthermore, there is a plateau of constant $m_{\rm max} \approx 25\,{\rm M}_\odot$ for clusters with masses between 1000 and 4000 M$_\odot$.

(i) $M_{\rm ecl} < 100\,{\rm M}_\odot$: the percentage of stars between the 1/6th and 5/6th quantiles is 89 per cent (83 per cent when taking the error bars into account) which is too tight for random sampling (66 per cent). Such a distribution is highly unlikely with a chance of only 0.2 per cent (0.1 per cent with errors) when calculated from a Binomial distribution. But the distribution around the median and the Wilcoxon singed-rank test are compatible with random sampling at a significance of 2 per cent.

(ii) $100 < M_{\rm ecl} \leq 1000\,{\rm M}_\odot$: 77 per cent (70 per cent with errors) of the stars are within the 1/6th and 5/6th quantiles which is somewhat tighter than expected for random sampling (66 per cent). The probability of this to occur is rather high with 8 per cent (13 per cent with errors). But 87 per cent of all clusters are below the random-sampling median where only 50 per cent would be expected and the Wilcoxon singed-rank test gives a very low probability (1.9×10^{-7}) that the data are distributed symmetrically around the median.

(iii) $M_{\rm ecl} > 1000\,{\rm M}_\odot$: only 12 per cent of the data points (66 per cent with errors) are in the 2/3rd interval which is far below the expectation from random sampling (66 per cent). The probability for a random occurrence of such a low number with the 2/3rd interval is 4×10^{-11}. Furthermore 97 per cent of the data points are lower than the median and the Wilcoxon singed-rank test results in a very low probability (2.8×10^{-9}) for a symmetric distribution, too.

The clusters in the mass range below 100 M$_\odot$ are the ones most compatible with the hypothesis of being randomly sampled from the IMF. This is also roughly the range of clusters studied by Maschberger & Clarke (2008). Their result, that the most-massive stars in these clusters could be randomly drawn from a universal IMF, is therefore in accordance with our conclusions. The difference is that here it is shown that this assumption cannot be generalized for more massive/richer clusters.

Selman & Melnick (2008) argue that the claim reached by Weidner & Kroupa (2006), that there exists a $m_{\rm max}$–$M_{\rm ecl}$ relation, is due to a size-of-sample effect in the data used by Weidner & Kroupa (2006). We now apply their analyses to our new data set. In appendix A of their paper, they use a method of adding up some clusters of the Weidner & Kroupa (2006) sample to so-called 'superclusters' of the same mass as NGC 6530 (about 1000 M$_\odot$ in the new sample presented here). By comparing the mean mass of the synthetic superclusters with the most-massive star of the component clusters, they show that there is no trend for the most-massive stars to be more massive with cluster mass. Here, we repeat the same method with our new sample of clusters. All possible combinations to reach the mass of NGC 6530 from within the sample are used and the most-massive star is plotted over the mean cluster mass, $\langle M_{\rm ecl}\rangle$, in Fig. 12. As is seen in the figure, the mass of the most-massive star increases with $\langle M_{\rm ecl}\rangle$. The Selman & Melnick (2008) explanation for the Weidner & Kroupa (2006) result therefore fails for the new sample.

These results strongly suggest an underlying physical $m_{\rm max}$–$M_{\rm ecl}$ relation. They contradict the hypothesis that star clusters are populated with stars by random sampling from the IMF. Only when taking into account the full range of the error bars *and* a very unlikely low fundamental upper mass limit of $m_{\rm max*} = 50\,{\rm M}_\odot$ would the complete sample mostly agree with random sampling. But in such a case, no stars above 50 M$_\odot$ would exist, a result clearly disproved by the dynamical mass measurements for the massive stars in Westerlund 2 and NGC 3603 (see Table 1).

The general trend of the most-massive star with cluster mass and the observed plateau between the two cluster mass regimes

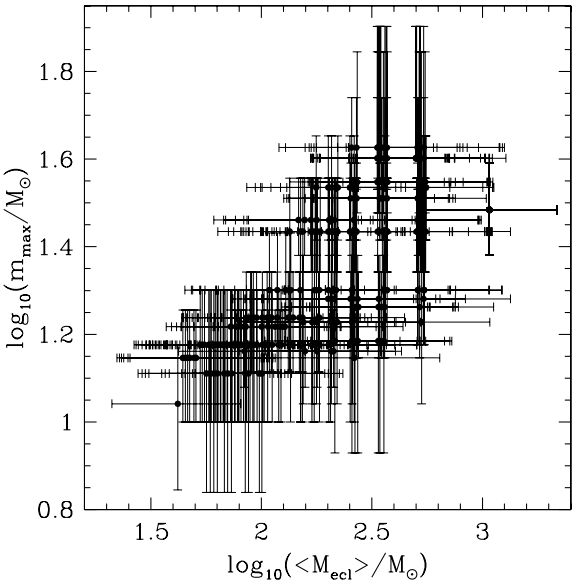

Figure 12. The mass of the most-massive star versus the mean mass of the so-called 'superclusters' constructed as in Selman & Melnick (2008). It shows whether or not the observed clusters of higher masses can be made by adding up large numbers of low-mass clusters. The obvious trend of increasing $m_{\rm max}$ with $<M_{\rm ecl}>$ is a clear indication against such a conclusion.

is therefore most likely a general result of the star-formation process within cluster-forming molecular cloud cores. Several different mechanisms might be responsible for the non-random behaviour of the formation of the most-massive star in star clusters. One such model is explored in Section 3.5, where the velocity dispersion within the cluster-forming cloud core is used as a measure for the binding energy of the cloud, and is compared with typical velocities of ionized gas which acts as a proxy for the radiative feedback of the stars. This simple model is already in qualitative agreement with the data, but more detailed studies of how the radiative and mechanical feedback of massive stars scales differently than the binding energy are needed. This may result in a critical $M_{\rm ecl}$ limit at which the one dominates over the other.

Another possible explanation for the existence of an $m_{\rm max}$–$M_{\rm ecl}$ relation might be given by dry mergers. In this scenario, massive stars form in smaller subclusters which are quickly evacuated by their feedback and these subclusters then merge nearly gas free, allowing only for very little additional accretion, that is mass growth. Only for initially very massive giant molecular clouds, more gas might be accreted during and after the merging of the subclusters.

The interesting split of the massive clusters into a tight and a loose subset by Pfalzner (2009, see Section 3.4) can be used as an additional constraint on the $m_{\rm max}$–$M_{\rm ecl}$ relation. The loose cluster stars form predominately by free-fall collapse of dense cores with little or no further gas accretion into the cluster. For the tight (high-density) clusters, cluster potential assisted accretion is possible which allows for more massive stars to form in these objects. Also stellar collisions, mergers and competitive accretion might play a role in these dense clusters.

A more detailed study of the possible mechanisms to explain the here presented observational evidence for a physical relation between $m_{\rm max}$ and $M_{\rm ecl}$ will be presented in a follow-on paper.

As the high-mass regime is most important for the question whether the integrated IMF of a galaxy is similar to the IMF derived locally on star cluster scales or not, this discardation of random sampling naturally leads the IGIMF being steeper than expected from individual star clusters. Since the majority of stars seem to form in star clusters but also these clusters are distributed according to a mass function which is dominated by lower mass clusters, the apparent non-randomness of these clusters lead to fewer OB stars per star in a galaxy than expected from random sampling.[7]

ACKNOWLEDGMENTS

We thank Jan Pflamm-Altenburg and Thomas Maschberger for several lengthy discussions on statistical methods. We also thank Vasili Gvaramadze for pointing out the work of Martins et al. (2005) on the recalibration of the masses of massive stars and Nick Moekel for further discussions. This work made use of the Webda and the Simbad web based data bases. This work was financially supported by the Chilean FONDECYT grant 3060096 and the CONSTELLATION European Commission Marie Curie Research Training Network (MRTN-CT-2006-035890).

REFERENCES

Adams F. C., Myers P. C., 2001, ApJ, 553, 744
Allen L. et al., 2007, in Reipurth B., Jewitt D., Keil K., eds, Protostars and Planets V. Univ. Arizona Press, Tucson, p. 361
Apai D., Bik A., Kaper L., Henning T., Zinnecker H., 2007, ApJ, 655, 484
Ascenso J., Alves J., Vicente S., Lago M. T. V. T., 2007, A&A, 476, 199
Aspin C., 2003, AJ, 125, 1480
Bastian N., Goodwin S. P., 2006, MNRAS, 369, L9
Bell E. F., McIntosh D. H., Katz N., Weinberg M. D., 2003, ApJS, 149, 289
Bhattacharyya G. K., Johnson R. A., 1977, Statistical Concepts and Methods. Wiley & Sons, New York
Blanco V. M., Williams A. D., 1959, ApJ, 130, 482
Bohigas J., Tapia M., 2003, AJ, 126, 1861
Bohigas J., Tapia M., Roth M., Ruiz M. T., 2004, AJ, 127, 2826
Bonanos A. Z. et al., 2004, ApJ, 611, L33
Bonatto C., Bica E., 2009, MNRAS, 394, 2127
Bonatto C., Santos J. F. C. Jr, Bica E., 2006, A&A, 445, 567
Bonnell I. A., Bate M. R., 2006, MNRAS, 370, 488
Bonnell I. A., Bate M. R., Zinnecker H., 1998, MNRAS, 298, 93
Bonnell I. A., Bate M. R., Vine S. G., 2003, MNRAS, 343, 413
Bonnell I. A., Vine S. G., Bate M. R., 2004, MNRAS, 349, 735
Borissova J., Ivanov V. D., Hanson M. M., Georgiev L., Minniti D., Kurtev R., Geisler D., 2008, A&A, 488, 151
Bosch G., Terlevich E., Terlevich R., 2009, AJ, 137, 3437
Bouy H. et al., 2009, A&A, 493, 931
Brandner W., 2008, in Beuther H., Linz H., Henning T., eds, ASP Conf. Ser. Vol. 387, Massive Star Formation: Observations Confront Theory. Astron. Soc. Pac., San Francisco, p. 369
Briceño C., Luhman K. L., Hartmann L., Stauffer J. R., Kirkpatrick J. D., 2002, ApJ, 580, 317
Carpenter J. M., Snell R. L., Schloerb F. P., 1990, ApJ, 362, 147
Carpenter J. M., Snell R. L., Schloerb F. P., Skrutskie M. F., 1993, ApJ, 407, 657
Carpenter J. M., Meyer M. R., Dougados C., Strom S. E., Hillenbrand L. A., 1997, AJ, 114, 198
Chabrier G., 2003, PASP, 115, 763
Chabrier G., Gallardo J., Baraffe I., 2007, A&A, 472, L17
Chen L., de Grijs R., Zhao J. L., 2007, AJ, 134, 1368
Cichowolski S., Romero G. A., Ortega M. E., Cappa C. E., Vasquez J., 2009, MNRAS, 394, 900
Clarke C. J., Pringle J. E., 1992, MNRAS, 255, 423

[7] The IGIMF concept is discussed in great detail in Kroupa & Weidner (2003) and Weidner & Kroupa (2005) and subsequent papers.

Cohen M., Kuhi L. V., 1979, ApJS, 41, 743
Crowther P. A., 2007, ARA&A, 45, 177
Dabringhausen J., Hilker M., Kroupa P., 2008, MNRAS, 386, 864
Dahm S. E., 2008, in Reipurth B., ed., ASP Monograph Publ. Vol. 4, Handbook of Star Forming Regions: Vol. I, The Northern Sky. Astron. Soc. Pac., San Francisco, p. 966
Dahm S. E., Hillenbrand L. A., 2007, AJ, 133, 2072
Dambis A. K., 1999, Astron. Lett., 25, 10
Damiani F., Flaccomio E., Micela G., Sciortino S., Harnden F. R., Murray S. S., 2004, ApJ, 608, 781
Damiani F., Prisinzano L., Micela G., Sciortino S., 2006, A&A, 459, 477
De Becker M., Rauw G., Manfroid J., Eenens P., 2006, A&A, 456, 1121
de Wit W. J., Testi L., Palla F., Vanzi L., Zinnecker H., 2004, A&A, 425, 937
de Wit W. J., Testi L., Palla F., Zinnecker H., 2005, A&A, 437, 247
Depoy D. L., Lada E. A., Gatley I., Probst R., 1990, ApJ, 356, L55
Diehl R. et al., 2006, Nat, 439, 45
Drew J. E., Busfield G., Hoare M. G., Murdoch K. A., Nixon C. A., Oudmaijer R. D., 1997, MNRAS, 286, 538
Elmegreen B. G., 1983, MNRAS, 203, 1011
Elmegreen B. G., 1999, ApJ, 515, 323
Elmegreen B. G., 2000, ApJ, 539, 342
Elmegreen B. G., 2006, ApJ, 648, 572
Faustini F., Molinari S., Testi L., Brand J., 2009, A&A, 503, 801
Figer D. F., 2005, Nat, 434, 192
Figer D. F., Kim S. S., Morris M., Serabyn E., Rich R. M., McLean I. S., 1999, ApJ, 525, 750
Figer D. F., Najarro F., Geballe T. R., Blum R. D., Kudritzki R. P., 2005, ApJ, 622, L49
Figer D. F. et al., 2002, ApJ, 581, 258
Forte J. C., Orsatti A. M., 1984, ApJS, 56, 211
Froebrich D., Meusinger H., Scholz A., 2008, MNRAS, 390, 1598
García B., Mermilliod J. C., 2001, A&A, 368, 122
Garmany C. D., Conti P. S., Massey P., 1980, ApJ, 242, 1063
Garmany C. D., Walborn N. R., 1987, PASP, 99, 240
Getman K. V., Feigelson E. D., Townsley L., Bally J., Lada C. J., Reipurth B., 2002, ApJ, 575, 354
Goodwin S. P., 1997, MNRAS, 284, 785
Goodwin S. P., Bastian N., 2006, MNRAS, 373, 752
Guetter H. H., Turner D. G., 1997, AJ, 113, 2116
Gutermuth R. A., Megeath S. T., Muzerolle J., Allen L. E., Pipher J. L., Myers P. C., Fazio G. G., 2004, ApJS, 154, 374
Gutermuth R. A., Megeath S. T., Pipher J. L., Williams J. P., Allen L. E., Myers P. C., Raines S. N., 2005, ApJ, 632, 397
Gutermuth R. A. et al., 2008, ApJ, 674, 336
Gvaramadze V. V., Bomans D. J., 2008, A&A, 490, 1071
Haisch K. E. Jr, Lada E. A., Lada C. J., 2000, AJ, 120, 1396
Hanson M. M., Howarth I. D., Conti P. S., 1997, ApJ, 489, 698
Harayama Y., 2007, PhD thesis, LMU, Munich, Germany
Harayama Y., Eisenhauer F., Martins F., 2008, ApJ, 675, 1319
Hasan P., Hasan S. N., Shah U., 2008, Ap&SS, 318, 25
Heske A., Wendker H. J., 1984, A&AS, 57, 205
Hillenbrand L. A., Hartmann L. W., 1998, ApJ, 492, 540
Hillenbrand L. A., Strom S. E., Vrba F. J., Keene J., 1992, ApJ, 397, 613
Hillenbrand L. A., Strom S. E., Calvet N., Merrill K. M., Gatley I., Makidon R. B., Meyer M. R., Skrutskie M. F., 1998, AJ, 116, 1816
Hurley J. R., 2003, in Makino J., Hut P., eds, IAU Symp. Vol. 208, Astrophysical Supercomputing using Particle Simulations. Astron. Soc. Pacific, San Francisco, p. 113
Jeffries R. D., Naylor T., Walter F. M., Pozzo M. P., Devey C. R., 2009, MNRAS, 393, 538
Kaas A. A. et al., 2004, A&A, 421, 623
Kiminki D. C. et al., 2007, ApJ, 664, 1102
Knödlseder J., 2000, A&A, 360, 539
Koen C., 2006, MNRAS, 365, 590
Koenig X. P., Allen L. E., Gutermuth R. A., Hora J. L., Brunt C. M., Muzerolle J., 2008, ApJ, 688, 1142
Kraus S. et al., 2009, A&A, 497, 195
Kroupa P., 1995, MNRAS, 277, 1491
Kroupa P., 2001, MNRAS, 322, 231
Kroupa P., 2002, Sci, 295, 82
Kroupa P., Weidner C., 2003, ApJ, 598, 1076
Kroupa P., Aarseth S., Hurley J., 2001, MNRAS, 321, 699
Kroupa P., Bouvier J., Duchêne G., Moraux E., 2003, MNRAS, 346, 354
Krumholz M. R., Klein R. I., McKee C. F., Offner S. S. R., Cunningham A. J., 2009, Sci, 323, 754
Lada E. A., Lada C. J., 1995, AJ, 109, 1682
Lada C. J., Lada E. A., 2003, ARA&A, 41, 57
Lada C. J., Margulis M., Dearborn D., 1984, ApJ, 285, 141
Lada E. A., Depoy D. L., Evans N. J. II, Gatley I., 1991, ApJ, 371, 171
Larson R. B., 1982, MNRAS, 200, 159
Larson R. B., 2002a, in Grebel E. K., Brandner W., eds, ASP Conf. Ser. Vol. 285, Modes of Star Formation and the Origin of Field Populations. Astron. Soc. Pac., San Francisco, p. 442
Larson R. B., 2002b, MNRAS, 332, 155
Larson R. B., 2003, ASP Conf. Ser. Vol. 287, Galactic Star Formation Across the Stellar Mass Spectrum. Astron. Soc. Pac., San Francisco, p. 65
Lata S., Pandey A. K., Sagar R., Mohan V., 2002, A&A, 388, 158
Liermann A., Hamann W.-R., Oskinova L. M., 2009, A&A, 494, 1137
Lucy L. B., 2006, A&A, 457, 629
Luhman K. L., 2008, in Reipurth B., ed., ASP Monograph Publ. Vol. 5, Handbook of Star Forming Regions: Vol. II, The Southern Sky. Astron. Soc. Pac., San Francisco, p. 169
MacConnell D. J., 1968, ApJS, 16, 275
Maíz Apellániz J., 2008, ApJ, 677, 1278
Maíz Apellániz J., 2009, ApJ, 699, 1938
Maíz Apellániz J., Walborn N. R., Morrell N. I., Niemela V. S., Nelan E. P., 2007, ApJ, 660, 1480
Marco A., Negueruela I., 2009, A&A, 493, 79
Martins F., Plez B., 2006, A&A, 457, 637
Martins F., Schaerer D., Hillier D. J., 2005, A&A, 436, 1049
Martins F., Hillier D. J., Paumard T., Eisenhauer F., Ott T., Genzel R., 2008, A&A, 478, 219
Maschberger T., Clarke C. J., 2008, MNRAS, 391, 711
Massey P., 1998, in Gilmore G., Howell D., eds, ASP Conf. Ser. Vol. 142, The Stellar Initial Mass Function. Astron. Soc. Pac., San Francisco, p. 17
Massey P., 2002, ApJS, 141, 81
Massey P., 2003, ARA&A, 41, 15
Massey P., Hunter D. A., 1998, ApJ, 493, 180
Massey P., Johnson J., 1993, AJ, 105, 980
Massey P., Silkey M., Garmany C. D., Degioia-Eastwood K., 1989, AJ, 97, 107
Massey P., Johnson K. E., Degioia-Eastwood K., 1995, ApJ, 454, 151
Massey P., DeGioia-Eastwood K., Waterhouse E., 2001, AJ, 121, 1050
Mayne N. J., Naylor T., Littlefair S. P., Saunders E. S., Jeffries R. D., 2007, MNRAS, 375, 1220
Menten K. M., Reid M. J., Forbrich J., Brunthaler A., 2007, A&A, 474, 515
Meynet G., Maeder A., 2003, A&A, 404, 975
Meynadier F., Heydari-Malayeri M., Walborn N. R., 2005, A&A, 436, 117
Miller G. E., Scalo J. M., 1979, ApJS, 41, 513
Morrell N. I. et al., 2001, MNRAS, 326, 85
Muno M. P. et al., 2006, ApJ, 636, L41
Naylor T., Fabian A. C., 1999, MNRAS, 302, 714
Nazé Y., Rauw G., Manfroid J., 2008, A&A, 483, 171
Negueruela I., Marco A., 2008, A&A, 492, 441
Negueruela I., Marco A., Herrero A., Clark J. S., 2008, A&A, 487, 575
Nelan E. P., Walborn N. R., Wallace D. J., Moffat A. F. J., Makidon R. B., Gies D. R., Panagia N., 2004, AJ, 128, 323
Neuhäuser R., Forbrich J., 2008, in Reipurth B., ed., ASP Monograph Publ. Vol. 5, Handbook of Star Forming Regions: Vol. II, The Southern Sky. Astron. Soc. Pac., San Francisco, p. 735
Niemela V., Gamen R., 2004, New Astron. Rev., 48, 727
Niemela V. S., Morrell N. I., Fernández Lajús E., Barbá R., Albacete Colombo J. F., Orellana M., 2006, MNRAS, 367, 1450
Oey M. S., Clarke C. J., 2005, ApJ, 620, L43

Oey M. S., King N. L., Parker J. W., 2004, AJ, 127, 1632
Ortolani S., Bonatto C., Bica E., Momany Y., Barbuy B., 2008, New Astron., 13, 508
Pandey A. K., Bhatt B. C., Mahra H. S., Sagar R., 1989, MNRAS, 236, 263
Pandey A. K., Sharma S., Ogura K., Ojha D. K., Chen W. P., Bhatt B. C., Ghosh S. K., 2008, MNRAS, 383, 1241
Park B.-G., Sung H., 2002, AJ, 123, 892
Parker R. J., Goodwin S. P., 2007, MNRAS, 380, 1271
Parker J. W., Zaritsky D., Stecher T. P., Harris J., Massey P., 2001, AJ, 121, 891
Paunzen E., Netopil M., Zwintz K., 2007, A&A, 462, 157
Pellerin A., Meyer M., Harris J., Calzetti D., 2006, in Combes F., Palous J., eds, IAU Symp. 235, Galaxy Evolution Across the Humble Time. Cambridge Univ. Press, Cambridge, p. 128
Penny L. R., Gies D. R., Hartkopf W. I., Mason B. D., Turner N. H., 1993, PASP, 105, 588
Pfalzner S., 2009, A&A, 498, L37
Pflamm-Altenburg J., Kroupa P., 2006, MNRAS, 373, 295
Pflamm-Altenburg J., Kroupa P., 2008, Nat, 455, 641
Pigulski A., Kolaczkowski Z., Kopacki G., 2000, Acta Astron., 50, 113
Piskunov A. E., Belikov A. N., Kharchenko N. V., Sagar R., Subramaniam A., 2004, MNRAS, 349, 1449
Pozzo M., Naylor T., Jeffries R. D., Drew J. E., 2003, MNRAS, 341, 805
Preibisch T., Zinnecker H., 2001, AJ, 122, 866
Preibisch T., Balega Y. Y., Schertl D., Weigelt G., 2002, A&A, 392, 945
Prisinzano L., Damiani F., Micela G., Sciortino S., 2005, A&A, 430, 941
Rathborne J. M., Jackson J. M., Simon R., 2006, ApJ, 641, 389
Rauw G., De Becker M., 2008, in Reipurth B., ed., ASP Monograph Publ. Vol. 5, Handbook of Star Forming Regions: Vol. II, The Southern Sky. Astron. Soc. Pac., San Francisco, p. 497
Rauw G., De Becker M., Gosset E., Pittard J. M., Stevens I. R., 2003, A&A, 407, 925
Ribas I., Morales J. C., Jordi C., Baraffe I., Chabrier G., Gallardo J., 2008, Mem. Soc. Astron. Ital., 79, 562
Rodney S. A., Reipurth B., 2008, in Reipurth B., ed., ASP Monograph Publ. Vol. 5, Handbook of Star Forming Regions: Vol. II, The Southern Sky. Astron. Soc. Pac., San Francisco, p. 633
Roman-Lopes A., 2007, A&A, 471, 813
Roman-Lopes A., Abraham Z., 2004, AJ, 128, 2364
Roman-Lopes A., Abraham Z., 2006, AJ, 131, 951
Roman-Lopes A., Abraham Z., Lépine J. R. D., 2003, AJ, 126, 1896
Salpeter E. E., 1955, ApJ, 121, 161
Sana H., Gosset E., Rauw G., Sung H., Vreux J.-M., 2006, A&A, 454, 1047
Sana H., Rauw G., Sung H., Gosset E., Vreux J.-M., 2007, MNRAS, 377, 945
Sana H., Gosset E., Nazé Y., Rauw G., Linder N., 2008, MNRAS, 386, 447
Sanchawala K. et al., 2007, ApJ, 667, 963
Scheepmaker R. A., Haas M. R., Gieles M., Bastian N., Larsen S. S., Lamers H. J. G. L. M., 2007, A&A, 469, 925
Schilbach E., Röser S., 2008, A&A, 489, 105
Schnurr O., Casoli J., Chené A.-N., Moffat A. F. J., St-Louis N., 2008, MNRAS, 389, L38
Schnurr O., Chené A.-N., Casoli J., Moffat A. F. J., St-Louis N., 2009, MNRAS, 397, 2049
Sellgren K., 1983, AJ, 88, 985
Selman F. J., Melnick J., 2008, ApJ, 689, 816
Selman F., Melnick J., Bosch G., Terlevich R., 1999, A&A, 347, 532
Sherry W. H., Walter F. M., Wolk S. J., 2004, AJ, 128, 2316
Silkey M., Massey P., 1986, BAAS, 18, 910
Sirianni M., Nota A., Leitherer C., De Marchi G., Clampin M., 2000, ApJ, 533, 203
Sirianni M., Nota A., De Marchi G., Leitherer C., Clampin M., 2002, ApJ, 579, 275
Smith J., Bentley A., Castelaz M., Gehrz R. D., Grasdalen G. L., Hackwell J. A., 1985, ApJ, 291, 571
Sung H., Bessell M. S., Chun M.-Y., 2004, AJ, 128, 1684
Tan J. C., Krumholz M. R., McKee C. F., 2006, ApJ, 641, L121
Testi L., Palla F., Prusti T., Natta A., Maltagliati S., 1997, A&A, 320, 159
Testi L., Palla F., Natta A., 1998, A&AS, 133, 81
Testi L., Palla F., Natta A., 1999, A&A, 342, 515
Testor G., Lemaire J. L., Kristensen L. E., Field D., 2005, in Casoli F., Contini T., Hameury J. M., Pagani L., eds, SF2A-2005: Semaine de l'Astrophysique Francaise. EdP-Sciences, Les Ulis, p. 401
Thies I., Kroupa P., 2007, ApJ, 671, 767
Thies I., Kroupa P., 2008, MNRAS, 390, 1200
Tout C. A., Aarseth S. J., Pols O. R., Eggleton P. P., 1997, MNRAS, 291, 732
Turner D. G., 1985, ApJ, 292, 148
Turner N. H., ten Brummelaar T. A., Roberts L. C., Mason B. D., Hartkopf W. I., Gies D. R., 2008, AJ, 136, 554
Vacca W. D., Garmany C. D., Shull J. M., 1996, ApJ, 460, 914
Vallenari A., Richichi A., Carraro G., Girardi L., 1999, A&A, 349, 825
Walborn N. R., 1973, AJ, 78, 1067
Walborn N. R. et al., 2002, AJ, 123, 2754
Walker M. F., 1959, ApJ, 130, 57
Wang S., Looney L. W., 2007, ApJ, 659, 1360
Wang J., Townsley L. K., Feigelson E. D., Getman K. V., Broos P. S., Garmire G. P., Tsujimoto M., 2007, ApJS, 168, 100
Wang S., Looney L. W., Brandner W., Close L. M., 2008, ApJ, 673, 315
Weidner C., 2009, MNRAS, submitted
Weidner C., Kroupa P., 2004, MNRAS, 348, 187
Weidner C., Kroupa P., 2005, ApJ, 625, 754
Weidner C., Kroupa P., 2006, MNRAS, 365, 1333
Weidner C., Kroupa P., Nürnberger D. E. A., Sterzik M. F., 2007, MNRAS, 376, 1879
Weidner C., Kroupa P., Maschberger T., 2009, MNRAS, 393, 663
Wijers R. A. M. J., Davies M. B., Tout C. A., eds., 1996, Evolutionary Processes in Binary Stars. Kluwer, Dordrecht
Wilking B. A., Gagné M., Allen L. E., 2008, in Reipurth B., ed., ASP Monograph Publ. Vol. 5, Handbook of Star Forming Regions: Vol. II, The Southern Sky. Astron. Soc. Pac., San Francisco, p. 124
Wilking B. A., Lada C. J., Young E. T., 1989, ApJ, 340, 823
Wolff S. C., Strom S. E., Dror D., Venn K., 2007, AJ, 133, 1092
Wolk S. J., Bourke T. L., Vigil M., 2008, in Reipurth B., ed., ASP Monograph Publ. Vol. 5, Handbook of Star Forming Regions: Vol. II, The Southern Sky. Astron. Soc. Pac., San Francisco, p. 124
Wolk S. J., Spitzbart B. D., Bourke T. L., Alves J., 2006, AJ, 132, 1100
Wyse R. F. G., Gilmore G., Houdashelt M. L., Feltzing S., Hebb L., Gallagher J. S., Smecker-Hane T. A., 2002, New Astron., 7, 395
Yun J. L., Djupvik A. A., Delgado A. J., Alfaro E. J., 2008, A&A, 483, 209
Zhang F., Han Z., Li L., Hurley J. R., 2005, MNRAS, 357, 1088

APPENDIX A: THE STELLAR INITIAL MASS FUNCTION

The following multicomponent power-law IMF is used throughout the paper,

$$\xi(m) = k \begin{cases} k' \left(\frac{m}{m_{\rm H}}\right)^{-\alpha_0} & , m_{\rm low} \leq m < m_{\rm H}, \\ \left(\frac{m}{m_{\rm H}}\right)^{-\alpha_1} & , m_{\rm H} \leq m < m_0, \\ \left(\frac{m_0}{m_{\rm H}}\right)^{-\alpha_1} \left(\frac{m}{m_0}\right)^{-\alpha_2} & , m_0 \leq m < m_1, \\ \left(\frac{m_0}{m_{\rm H}}\right)^{-\alpha_1} \left(\frac{m_1}{m_0}\right)^{-\alpha_2} \left(\frac{m}{m_1}\right)^{-\alpha_3} & , m_1 \leq m < m_{\rm max}, \end{cases} \tag{A1}$$

with exponents

$$\begin{aligned} \alpha_0 &= +0.30, \quad 0.01 \leq m/{\rm M}_\odot < 0.08, \\ \alpha_1 &= +1.30, \quad 0.08 \leq m/{\rm M}_\odot < 0.50, \\ \alpha_2 &= +2.35, \quad 0.50 \leq m/{\rm M}_\odot < 1.00, \\ \alpha_3 &= +2.35, \quad 1.00 \leq m/{\rm M}_\odot < m_{\rm max}, \end{aligned} \tag{A2}$$

where $\mathrm{d}N = \xi(m)\,\mathrm{d}m$ is the number of stars in the mass interval m to $m + \mathrm{d}m$. The exponents α_i represent the standard or canonical IMF and have been corrected for unresolved multiple systems (Kroupa 2001, 2002; Thies & Kroupa 2007, 2008; Weidner et al. 2009). The advantage of such a multipart power-law description is the easy integrability and, more importantly, that different parts of the IMF can be changed readily without affecting other parts. Note that this form is a two-part power law in the stellar regime, and that brown dwarfs contribute about 4 per cent by mass only and need to be treated as a separate population such that the IMF has a discontinuity near $m_\mathrm{H} = 0.08\,\mathrm{M}_\odot$ with $k' \sim 1/3$ (Kroupa et al. 2003; Thies & Kroupa 2007, 2008). A log-normal form below $1\,\mathrm{M}_\odot$ with a power-law extension to high masses was suggested by Chabrier (2003) but is indistinguishable from the canonical form (Dabringhausen, Hilker & Kroupa 2008) and does not cater for the discontinuity. The canonical IMF is today understood to be an invariant Salpeter/Massey power-law slope (Salpeter 1955; Massey 2003) above $0.5\,\mathrm{M}_\odot$, being independent of the cluster density and metallicity for metallicities $Z \gtrsim 0.002$ (Massey & Hunter 1998; Sirianni et al. 2000, 2002; Parker et al. 2001; Massey 1998, 2002, 2003; Larson 2002a,b; Wyse et al. 2002; Bell et al. 2003; Piskunov et al. 2004; Pflamm-Altenburg & Kroupa 2006).

The basic assumption underlying our approach is the notion that all stars in every cluster are drawn from this same universal parent IMF, which is consistent with observational evidence (Elmegreen 1999; Kroupa 2001).

It should be noted here that, while not indicated in equation (A2), there is evidence of a maximal mass for stars ($m_\mathrm{max} \leq m_\mathrm{max*} \approx 150\mathrm{M}_\odot$; Weidner & Kroupa 2004), a result confirmed by several independent studies (Figer 2005; Oey & Clarke 2005; Koen 2006).

APPENDIX B: THE CLUSTER SAMPLE

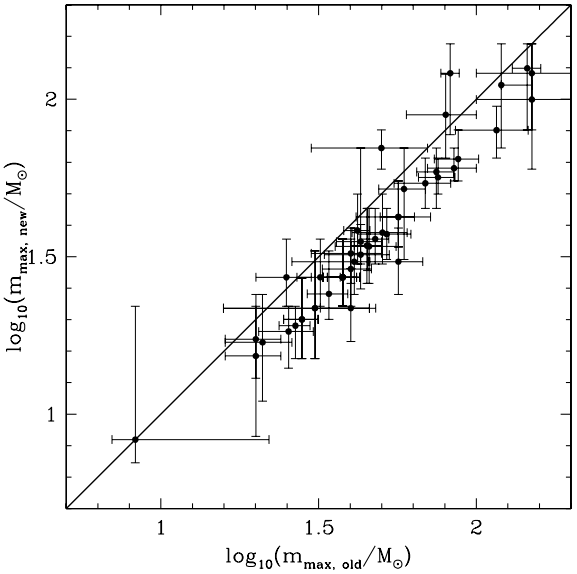

Figure B1. The values for the O-star masses from the old calibration on the abscissa versus the newly calibrated ones on the ordinate. The thick solid line indicates were both values would be the same.

Table B1. Literature data for the empirical cluster masses ($M_{\rm ecl}$), maximal star masses ($m_{\rm max,obs}$) within these clusters, cluster ages (age), distances (D), the numbers of stars above or within certain mass limits (in $M_\odot$), the name and the spectral type of the most-massive star and references for the data.

Designation	$M_{\rm ecl}$ ($M_\odot$)	$m_{\rm max\ obs\ old}$ ($M_\odot$)	$m_{\rm max\ obs\ new}$ ($M_\odot$)	Age (Myr)	D (pc)	No. of stars	Id $m_{\rm max}$	Sp Type	Ref.
IRAS 05274+3345	14 −7/+15	7.0 ± 2.5		1.0	1800	15 > 0.24	-	B2	(1)
Mol 139	16 ± 8	2.9 ± 2.0		<1	7300	-	-	-	(2)
Mol 143	21 ± 10	3.1 ± 2.0		<1	5000	-	-	-	(2)
IRAS 06308+0402	24 −13/+25	11.0 ± 4.0		1.0	1600	16 > 0.37	-	B0.5	(1)
VV Ser	25 −13/+27	3.3 ± 1.0		0.6	440	24 > 0.3	VV Ser	B9e	(3)
VY Mon	28 −15/+29	4.1 ± 1.0		0.1	800	26 > 0.3	VY Mon	B8e	(3)
Mol 8A	30 ± 15	3.8 ± 2.0		<1	11500	-	-	-	(2)
IRAS 05377+3548	30 −15/+32	9.5 ± 2.5		1.0	1800	31 > 0.24	-	B1	(1)
Ser SVS2	31 −16/+31	2.2 ± 0.2		2.0	259 ± 37	50 > 0.17	BD 01° 3689	A0	(4)
Tau-Aur	31 −18/+36	7.0 ± 2.5		1-2	140	123 > 0.02	HK Tau/G1	B2	(5)
IRAS 05553+1631	31 −16/+33	9.5 ± 2.5		1.0	2000	28 > 0.28	-	B1	(1)
IRAS 05490+2658	33 −17/+36	7.0 ± 2.5		1.0	2100	30 > 0.29	-	B2	(1)
IRAS 03064+5638	33 −17/+36	11.0 ± 4.0		1.0	2200	27 > 0.31	-	B0.5	(1)
IRAS 06155+2319	34 −18/+35	9.5 ± 2.5		1.0	1600	38 > 0.21	-	B1	(1)
Mol 50	36 ± 18	3.5 ± 2.0		<1	4900	-	-	-	(2)
Mol 11	47 ± 20	3.8 ± 2.0		<1	2100	-	-	-	(2)
IRAS 06058+2138	51 −27/+54	7.0 ± 2.5		1.0	2000	26 > 0.49	-	B2	(1)
NGC 2023	55 −28/+58	8.0 ± 2.0		3.0	400	21 > 0.6	HD 37903	B1.5V	(6)
Mol 3	61 ± 20	3.7 ± 2.0		<1	2170	-	-	-	(2)
Mol 160	63 ± 20	4.3 ± 2.0		<1	5000	-	-	-	(2)
NGC 7129	63 −33/+104	9.2 ± 3.0		0.1	1000	53 > 0.3/3 > 3	BD 65° 1637	B3e	(7)
IRAS 06068+2030	67 −35/+70	11.0 ± 4.0		1.0	2000	59 > 0.28	-	B0.5	(1)
IRAS 00494+5617	71 −37/+74	9.5 ± 2.5		1.0	2200	58 > 0.31	-	B1	(1)
IRAS 05197+3355	72 −38/+75	11.0 ± 4.0		1.0	3200	34 > 0.50	-	B0.5	(1)
Cha I	80 −46/+91	5.0 ± 3.0		2.0	170 ± 10	237 > 0.04	HD 96675	B6IV/V	(8)
V921 Sco	71 −36/+429	14.0 ± 4.0		0.1-1	800	33 > 0.5	V921 Sco	B0e	(7)
IRAS 05375+3540	73 −38/+78	11.0 ± 4.0		1.0	1800	74 > 0.24	-	B0.5	(1)
IRAS 02593+6016	78 −41/+81	15.0 ± 5.0		1.0	2200	61 > 0.31	-	B0	(1)
Mol 103	80 ± 20	4.0 ± 2.0		<1	4100	-	-	-	(2)
NGC 2071	80 −44/+89	4.0 ± 2.0		1.0	400	105 > 0.2	V1380 Ori	B5	(9)
MWC 297	85 ± 60	8.3 −1.3/+13.7	8.3 −1.3/+13.7	0.1-1	250 or 450	24 > 0.3	-	B1.5V or O9e	(3)
IC 348	89 −46/+92	6.0 ± 1.0		1.3	310	173 > 0.1	BD 31°643	B5V	(10)
BD 40° 4124	90 −49/+106	12.9 −6.0/+ 2.0		0.1-6	1000	74 > 0.3 / 3 > 3	BD 40° 4124	B2e	(3)
ρ Oph	91 −46/+93	8.0 ± 1.0		0.1-1	130 ± 20	78 > 0.3	ρ Oph	BIV	(11)
IRAS 06056+2131	92 −49/+97	7.0 ± 2.5		1.0	2000	85 > 0.28	-	B2	(1)
IRAS 05100+3723	98 −51/+103	15.0 ± 5.0		1.0	2600	63 > 0.38	-	B0	(1)
R CrA	105 −55/+114	4.0 ± 2.0		1.0	130	55 > 0.5	R CrA	A5eII	(12)
NGC 1333	105 −54/+111	5.0 ± 1.0		1-3	250	134 > 0.2	SSV 13	-	(13)
Mol 28	105 ± 20	9.9 ± 2.0		<1	4500	-	-	-	(2)
IRAS 02575+6017	111 −57/+116	9.5 ± 2.5		1.0	2200	91 > 0.31	-	B1	(1)
W40	144 −80/+576 100	10.0 ± 5.0		1-2	600	3 > 4	IRS 2a	-	(14)
σ Ori	150 −76/+155	20.0 ± 4.0	17.3 −4.3/+4.7	2.5	360 ± 60	140 ± 10 (0.2-1.0)	σ Ori A	O9-9.5V	(15)
NGC 2068	151 −86/+169	5.0 ± 3.0		1.0	400	192 > 0.2	HD 38563A	B4V	(16)
NGC 2384	189 −95/+192	16.5 ± 1.5		1.0	2100	7 > 3	HD 58509	B0.5III	(17)

Table B1 – *continued*

Designation	$M_{\rm ecl}$ ($M_\odot$)	$m_{\rm max\,obs\,old}$ ($M_\odot$)	$m_{\rm max\,obs\,new}$ ($M_\odot$)	Age (Myr)	D (pc)	No. of stars	Id $m_{\rm max}$	Sp Type	Ref.
Mon R2	225 −117/+236	15.0 ± 5.0		0-3	830 ± 50	309 > 0.15	IRS 1SW	B0	(18)
IRAS 06073+1249	239 −120/+242	11.0 ± 4.0		1.0	4800	25 > 1.47	-	B0.5	(1)
Trumpler 24	251 −131/+291	14.5 ± 2.5		1.0	1140	4 > 5	GSC 7872-1609	WN	(19)
IC 5146	293 −226/+305	14.0 ± 4.0		1.0	900	238 > 0.3/5 > 3	BD 46° 3474	B0e	(20)
HD 52266	400 ± 350	28.0 ± 3.5	20.0 −5.0/+7.0	<3.0	1700 ± 1000	4 ± 2 > 4	HD 52266	O8-9V	(21)
HD 57682	400 ± 350	28.0 ± 3.5	20.0 −5.0/+7.0	<3.0	?	4 ± 5 > 4	HD 57682	O8-9V	(21)
Alicante 5	461 −234/+516	12.0 ± 4.0		<3.0	3600 +600/-400	22 > 2.5	A47	B0.7V	(22)
Cep OB3b	485 −243/+497	37.7 ± 5.0	27.2 −5.2/+8.8	3.0	800 ± 100	12 > 4	HD 217086	O7Vn	(23)
HD 153426	500 ± 350	40.0 ± 6.5	28.9 −6.9/+7.1	<3.0	?	5 ± 4 > 4	HD 153426	O6.5-7V	(21)
NGC 2264	525 −267/+537	25.0 ± 5.0	27.2 −5.2/+8.8	3.0	760 ± 100	1000 > 0.08	S Mon / HD 47839	O7Ve	(24)
Sh2-294	525 −267/+540	12.5 ± 2.5		4.0	3200	155 > 0.7	S294B0.5V	B0.5V	(25)
RCW 116B	536 −276/557	21.0 ± 5.0	16.9 −5.9/+7.1	2.5	1100	102 > 0.95	-	B1V-O8V	(26)
NGC 6383	561 −281/+563	37.7 ± 5.0	27.2 −5.2/+8.8	2.0	1300 ± 100	21 > 3	HD 159176	O7V + O7V	(27)
Alicante 1	577 −290/+583	45.0 ± 5.0	34.3 −8.3/+10.7	2-3	4000 ± 400	38 > 2.0	BD 56° 864	O6V	(28)
HD 52533	621 −417/+1077	26.7 ± 3.0	19.1 −4.1/+2.9	<3.0	?	15 ± 5 > 4	HD 52533	O8.5-9V	(21)
Sh2-128	666 −342/+736	37.7 ± 5.0	27.2 −5.2/+8.8	2.0	9400	7 > 7	-	O7V	(29)
NGC 2024	690 −350/+706	20.0 ± 4.0	15.3 −6.8/+8.7	0.5	400	309 > 0.5	IRS 2b	O8V − B2V	(30)
HD 195592	725 −364/+757	40.0 ±10.0	32.4 −6.4/+6.6	<3.0	?	18 ± 3 > 4	HD 195592	O6-6.5V	(21)
Sh2-173	748 −395/+901	25.4 ± 5.0	18.3 −4.3/+3.7	0.6-1.0	2500 ± 500	7 > 7	BD 60° 39	O9V	(31)
DBSB 48	792 −416/+1126	56.6 ± 15.0	42.3 −8.3/+12.7	1.1	5000 ± 700	5 > 10	-	O5V	(32)
NGC 2362	809 −409/+823	43.0 ± 7.0	35.3 −5.3/+34.7	3.0	1390 ± 200	353 > 0.5	τ CMa	O9Ib	(33)
Pismis 11	896 −448/+938	40.0 −0.0/+40.0		3-5	3600 +600/-400	43 > 2.5	HD 80077	B2Ia	(22)
NGC 6530	1075 −545/+1097	56.6 ± 11.0	30.5 −6.5/+8.5	2.3	1350 ± 200	620 > 0.4	HD 165052	O6.5V	(34)
FSR 1530	1410 −707/+1581	30.0 ± 15.0		<4.0	2750 ± 750	35 > 4	[M81]I-296	-	(35)
Berkeley 86	1440 −730/+1470	40.0 ± 8.0	21.7 −4.7/+7.3	3-4	1700	340 > 0.8	HD 193595	O8V(f)	(36)
NGC 637	1682 −854/+1726	30.8 ± 15.0	21.7 −6.7/+11.3	4.0	2160	$583M_\odot > 1.6$	-	≈O8	(37)
W5Wb	1734 −874/+1757	34.1 ± 5.0	24.1 −4.1/+8.9	2.0	2000	300 > 1	BD 60° 586	O7.5V	(38)
Stock 16	1857 −955/+2045	43.0 ± 10.0	32.1 −7.1/+7.9	4.0	1650	16 > 8	HD 115454	O7.5III	(39)
ONC	2124 −1078/+2175	35.8^a ± 7.2	34.3 − 5.7/+10.7	<1.0	414 ± 7	3500 (0.1 − 30)	Θ Orionis C1	O6Vpe	(40)
RCW 38	2251 −1132/+2276	50.4 ± 10.0	37.7 −7.7/+12.3	<1.0	1700	2000 > 0.25	IRS 2	O5.5V	(41)
Bochum 2	2284 −1302/+3523	37.7 ± 4.0	27.2 −5.2/+8.8	2-4	2700	4 > 16	BD 00° 1617B	O7V	(42)
Berkeley 59	2310 −1168/+2417	37.7 ± 4.0	27.2 −5.2/+8.8	2.0	1000	41 > 5	BD 66° 1675	O7V	(43)
IC 1590	2376 −1245/+2799	41.0 ± 5.2	30.5 −6.5/+8.5	3.5	2900	14 > 10	BD 55° 191	O6.5V	(44)
W5E	2614 −1323/+2667	37.7 ± 5.0	27.2 −5.2/+8.8	2.0	2000	400 − 500 > 1	HD 18326	O7V	(38)
W5Wa	2651 −1338/+2690	52.0 ± 10.0	37.3 −6.3/+7.7	2.0	2000	400 − 500 > 1	HD 17505	O6.5III	(38)
NGC 1931	3128 −1564/+3163	30.8 ± 15.0	21.7 −6.7/+11.4	4.0	3086	$848M_\odot > 2.39$	-	≈O8	(37)
LH 118	3746 −1918/+4077	56.6 ± 7.0	42.3 −8.3/+12.7	3.0	48500	28 > 9	LH 118-241	O5V	(45)
NGC 2103	3853 −1937/+3905	80.0 ± 20.0	89.3 −24.3/+30.7	1.0	48500	26 > 10	Sk −71° 51	O2V((f*))	(46)
NGC 7380	4527 −2290/+4611	47.8 ± 5.0	36.0 −6.0/+9.0	2.0	3700	42 (6–12)	HD 215835	O5.5-6V((f))	(47)
NGC 6231	4595 −2312/+4676	59.0 ± 10.0	51.9 −20.9/+18.1	1.0	1600	51 > 7	HD 152248	O7Ib	(48)
RCW 106	4681 −2375/+4871	45.7 ± 10.0	34.1 −8.1/+10.9	2.5	1100	41 > 8	-	O5.5-6.5V	(49)
NGC 6823	4983 −2584/+5685	37.7 ± 4.0	27.2 −5.2/+8.8	2-4	1900	42 > 8	BD 22° 3782	O7V(f)	(50)
RCW 121	5323 −2671/+5390	42.0 ± 4.0	38.3 −8.3/+11.7	4.2	1600	96 > 5	-	O6V-O5V	(51)

Table B1 – *continued*

Designation	$M_{\rm ecl}$ ($M_\odot$)	$m_{\rm max\,obs\,old}$ ($M_\odot$)	$m_{\rm max\,obs\,new}$ ($M_\odot$)	Age (Myr)	D (pc)	No. of stars	Id $m_{\rm max}$	Sp Type	Ref.
NGC 2244	$5946\ -3029/+6102$	68.9 ± 14.0	$54.1\ -9.1/+10.9$	1.9	1500	$54\,(6-12)$	HD 46223	O4V(f)	(52)
NGC 2122	$6764\ -3416/+6960$	74.7 ± 10.0	$58.8\ -13.8/+11.2$	3.0	48500	$52 > 9$	HD 270145	O6I(f)	(53)
[OBS 2003] 179	7000 ± 3500	50.0 ± 20.0	70.0 ± 10.0	2-5	7900	$10 > 16$	Obj 4	Ofpe/WN9	(54)
Westerlund 2	$8845\ -4456/+9009$	$82.7^a \pm 5.5$	$121.0\ -43.8/+29.0$	1-2	8000	$29 > 16.5$	WR20a A	WN6ha	(55)
RCW 95	$9670\ -4840/+9720$	87.6 ± 14.0	$64.6\ -9.6/+15.4$	1.5	2400	$136 > 6$	-	O3V	(56)
IC 1805	$10885\ -5528/+11137$	75.6 ± 10.0	$56.5\ -6.5/+8.5$	2.0	2350	$99\,(6-12)$	HD 15558	O4-5III(f)	(47)
NGC 6357	$11978\ -6430/+11979$	115.9 ± 30.0	$79.8\ -14.8/+15.2$	1.0	2560	$38 > 16.5$	HDE 319718A	O3If	(57)
NGC 3603	$1.3 \times 10^4 \pm 3000$	150.0 ± 50.0	$121.0\ -41.0/+29.0$	0.7	6000	-	NGC 3603-B	WN6ha	(58)
Trumpler 14/16	$17890\ -8945/+18676$	150.0 ± 50.0	$99.8\ -39.8/+50.2$	1.7	2500	$64 > 16$	η Carina	LBV	(59)
NGC 6611	$25310\ -12659/+25503$	85.0 ± 15.0	$60.4\ -5.6/+9.6$	1.3	1800	$460 > 5$	HD 168076	O4III	(60)
Cyg OB2	$75890\ -38453/+78716$	$92.0\ -25.0/+58.0$		2.0	1700	$8600 > 1.3$	Cyg OB2-12	B8Ia	(61)
Arches	$77225\ -39250/+77225$	$120.0\ -0.0/+30.0$	$111.0\ -41.0/+39.0$	2.5	7620	$196 > 20.1$	N4	WN7-8h	(62)
R 136	$222912\ -112104/+224426$	145.0 ± 15.0	$125.4\ -45.4/+24.6$	1-2	48500	$8000 > 3$	R136a1	O2If*/WN4.5	(63)

[a] Dynamical mass estimates from binary orbits exist for these stars.

Table B2. References for Table B1.

1:	Carpenter, Snell & Schloerb (1990), Carpenter et al. (1993),
2:	Faustini et al. (2009),
3:	Testi et al. (1997, 1998, 1999); Wang & Looney (2007),
4:	Kaas et al. (2004),
5:	Cohen & Kuhi (1979), Briceño et al. (2002),
6:	Sellgren (1983); Depoy et al. (1990); Lada et al. (1991),
7:	Gutermuth et al. (2004), Wang & Looney (2007),
8:	Luhman (2008),
9:	Lada et al. (1991),
10:	Preibisch & Zinnecker (2001), Lada & Lada (2003),
11:	Wilking, Lada & Young (1989), Larson (2003), Wilking, Gagné & Allen (2008),
12:	Neuhäuser & Forbrich (2008),
13:	Aspin (2003); Getman et al. (2002); Gutermuth et al. (2008),
14:	Smith et al. (1985), Rodney & Reipurth (2008),
15:	Sherry, Walter & Wolk (2004), Bouy et al. (2009),
16:	Sellgren (1983), Lada et al. (1991),
17:	Pandey et al. (1989),
18:	Carpenter et al. (1997), Preibisch et al. (2002),
19:	Heske & Wendker (1984), Pandey et al. (1989),
20:	Walker (1959); Forte & Orsatti (1984); Pandey et al. (1989); Wang & Looney (2007); Mayne et al. (2007),
21:	de Wit et al. (2004, 2005),
22:	Marco & Negueruela (2009),
23:	Naylor & Fabian (1999); Pozzo et al. (2003); Mayne et al. (2007),
24:	Sung, Bessell & Chun (2004), Mayne et al. (2007), Dahm (2008),
25:	Yun et al. (2008),
26:	Roman-Lopes (2007),
27:	Rauw et al. (2003), Paunzen, Netopil & Zwintz (2007), Rauw & De Becker (2008),
28:	Negueruela & Marco (2008),
29:	Bohigas & Tapia (2003),
30:	Lada et al. (1991), Haisch, Lada & Lada (2000), Sherry et al. (2004),
31:	Cichowolski et al. (2009),
32:	Ortolani et al. (2008),
33:	Mayne et al. (2007), Dahm & Hillenbrand (2007),
34:	Prisinzano et al. (2005); Damiani et al. (2004, 2006); Mayne et al. (2007), Chen, de Grijs & Zhao (2007),
35:	Froebrich, Meusinger & Scholz (2008),
36:	Massey, Johnson & Degioia-Eastwood (1995), Vallenari et al. (1999),
37:	Hasan, Hasan & Shah (2008),
38:	Koenig et al. (2008),
39:	Turner (1985), Pandey et al. (1989),
40:	Hillenbrand & Hartmann (1998); Hillenbrand et al. (1998); Menten et al. (2007); Kraus et al. (2009),
41:	Wolk et al. (2006), Wolk, Bourke & Vigil (2008),
42:	Dambis (1999), Lata et al. (2002),
43:	Blanco & Williams (1959); MacConnell (1968); Pandey et al. (2008),
44:	Walborn (1973); Guetter & Turner (1997); Lata et al. (2002),
45:	Massey et al. (1989),
46:	Meynadier, Heydari-Malayeri & Walborn (2005),
47:	Wolff et al. (2007),
48:	García & Mermilliod (2001); Sana et al. (2006, 2007, 2008),
49:	Roman-Lopes, Abraham & Lépine (2003), Roman-Lopes (2007),
50:	Pigulski, Kolaczkowski & Kopacki (2000), Lata et al. (2002),
51:	Roman-Lopes & Abraham (2006), Roman-Lopes (2007),
52:	Massey et al. (1995); Park & Sung (2002); Chen et al. (2007); Wolff et al. (2007); Bonatto & Bica (2009),
53:	Silkey & Massey (1986); Garmany & Walborn (1987); Massey et al. (1989); Niemela & Gamen (2004),
54:	Borissova et al. (2008),
55:	Bonanos et al. (2004), Nazé, Rauw & Manfroid (2008),
56:	Roman-Lopes & Abraham (2004), Roman-Lopes (2007),
57:	Bohigas et al. (2004); Maíz Apellániz et al. (2007); Wang et al. (2007),
58:	Harayama (2007), Harayama, Eisenhauer & Martins (2008), Schnurr et al. (2008),
59:	Penny et al. (1993); Massey & Johnson (1993); Massey et al. (1995); Nelan et al. (2004); Oey & Clarke (2005); Ascenso et al. (2007); Sanchawala et al. (2007); Ortolani et al. (2008),
60:	Bonatto, Santos & Bica (2006), Wolff et al. (2007),
61:	Knödlseder (2000), Massey, DeGioia-Eastwood & Waterhouse (2001), Wolff et al. (2007), Negueruela et al. (2008),
62:	Figer et al. (2002), Martins et al. (2008),
63:	Massey & Hunter (1998); Selman et al. (1999); Schnurr et al. (2009)

APPENDIX C: NOTES ON INDIVIDUAL STAR CLUSTERS

C1 MWC 297

Depending on the uncertain distance the spectral type of the brightest star is either O9e (450 pc; Hillenbrand et al. 1992) or B1.5V (250 pc; Drew et al. 1997). Wang & Looney (2007) assume the O9e spectral type and assign the star a mass of 26.5 $M_\odot$. This mass estimate is rather odd as older literature gives 22 (Hanson, Howarth & Conti 1997) or 25.4 (Vacca et al. 1996) $M_\odot$ for a O9 star and the new Martins et al. (2005) calibration yields 18 $M_\odot$. Here, we assume the newer distance of 250 pc and therefore the spectral type B1.5V but include the mass of an O9V star as an upper limit (22 $M_\odot$ for the old calibration and 18 $M_\odot$ for the new one).

C2 Pismis 11

It is not certain whether HD 80077 is part of this star cluster or not (Marco & Negueruela 2009). If it is, it would be one of the brightest stars in the MW. Because it is an evolved star (B2Ia), the precise initial mass is not known, only that it should be above 40 $M_\odot$.

C3 NGC 2244

Bonatto & Bica (2009) give a mass of 625 $M_\odot$ for this cluster from fitting a King profile to the MS and PMS stars they found. But when using the number of B0 to B3 stars (54 between 6 and 12 $M_\odot$ $M_\odot$) from Wolff et al. (2007), an IMF extrapolation yields a cluster mass of about 6000 $M_\odot$. A reason for this discrepancy is currently not known.

C4 γ Velorum Cluster

Jeffries et al. (2009) studied a group of several hundred PMS stars around the massive binary γ^2 Vel (WC8 + O7.5V) in the Vela OB2 association. They concluded that it is a young ($\approx$7 Myr) low-mass (250–360 $M_\odot$) cluster with a very massive star (initial mass for the WC8 star >40 $M_\odot$). This object has not been included because of its age and the possible mass loss from the cluster due to gas expulsion.

C5 Trumpler 14/16

Trumpler 14 and Trumpler 16 are believed to be one single cluster optically divided by a large patch of gas and dust (Oey & Clarke 2005). Some studies do not consider η Carina as part of this cluster. If η Car is not part of the cluster then the O3If* star HD 93129AB (67^+ $M_\odot$) would be the most-massive star in the cluster.

C6 Cyg OB2

The star Cyg OB2−12 is an evolved star (B8Ia) and is considered to be one of or maybe even the brightest star in the MW. Negueruela et al. (2008) estimate its initial mass with 92 $M_\odot$. The region contains 8600 stars earlier than F3, some 2600 OB stars and around 120 O-stars and has been described by Knödlseder (2000) as a possible young globular cluster within the MW disk.

C7 R 136

There is some debate in the literature whether or not extremely massive stars (>80 $M_\odot$) might or might not look like Wolf–Rayet stars even while they still burn hydrogen in their cores (Crowther 2007). Therefore, the spectral type of the most-massive star (R136a1) might be either O2If* or WN4.5. But this has little consequences for the mass estimate for this star as it is based on a detailed spectral analysis (Massey & Hunter 1998). The mass estimate for the cluster, 2.2×10^5 $M_\odot$, is for R 136 only. The cluster contains about 8000 stars between 3 and 120 $M_\odot$ and 39 O3If* stars. The whole region of 30 Doradus is believed to hold a total of 4.5×10^5 $M_\odot$ in stars (Bosch, Terlevich & Terlevich 2009).

C8 Cl 1806−20

The cluster and its most massive star, LBV 1806−20, one of the brightest stars in the MW, have not been included because the cluster is known to host a pulsar (SGR 1806−20) and is therefore most probably too old for the current study. Additionally, very little is known about its stellar population besides the LBV, the pulsar, an OB supergiant and three Wolf–Rayet stars as this cluster is on the far side of the Galaxy ($D \approx 15\,000$ pc) and heavily dust obscured (Figer et al. 2005).

C9 Quintuplet

This massive cluster ($\sim 1.2 \times 10^4$ $M_\odot$; Figer et al. 1999; Liermann, Hamann & Oskinova 2009) hosts the Pistol star which is one of the brightest and most massive stars in the Galaxy (150^+ $M_\odot$?) but is believed to be 4–6 Myr old and therefore too old for this study.

C10 Westerlund 1

Another massive cluster (>10^4 $M_\odot$; Brandner 2008) with about 150 O-stars. It houses an X-ray pulsar (Muno et al. 2006) and is therefore not included into this study as it is too old (4–5 Myr).

This paper has been typeset from a TEX/LATEX file prepared by the author.